Poster Setup and Presentation Times

Poster Setup

Sunday, June 17 ..... 8:00 AM–3:00 PM

Your poster must be set up by 3:00 PM on Sunday, June 17.

Poster Presentation Times

(Please plan to attend your posters during the following times).

Sunday, June 17 (Welcome Reception) .....6:00 PM–6:30 PM

Monday, June 18 .....10:00 AM–10:30 AM
.....*and* 3:00 PM–3:30 PM

Tuesday, June 19..... 9:55 AM–10:25 AM

Wednesday, June 20.....10:15 AM–10:45 AM

Young Investigator Judging Times

Monday, June 18. .....10:00 AM–10:30 AM
.....and 3:00 PM–3:30 PM

Tuesday, June 19..... 9:55 AM–10:25 AM

Poster Teardown

Wednesday, June 20..... 12:00 Noon–1:00 PM

Posters not removed by 1:00 pm, Wednesday, June 20, will be taken to the Registration Desk for pickup.

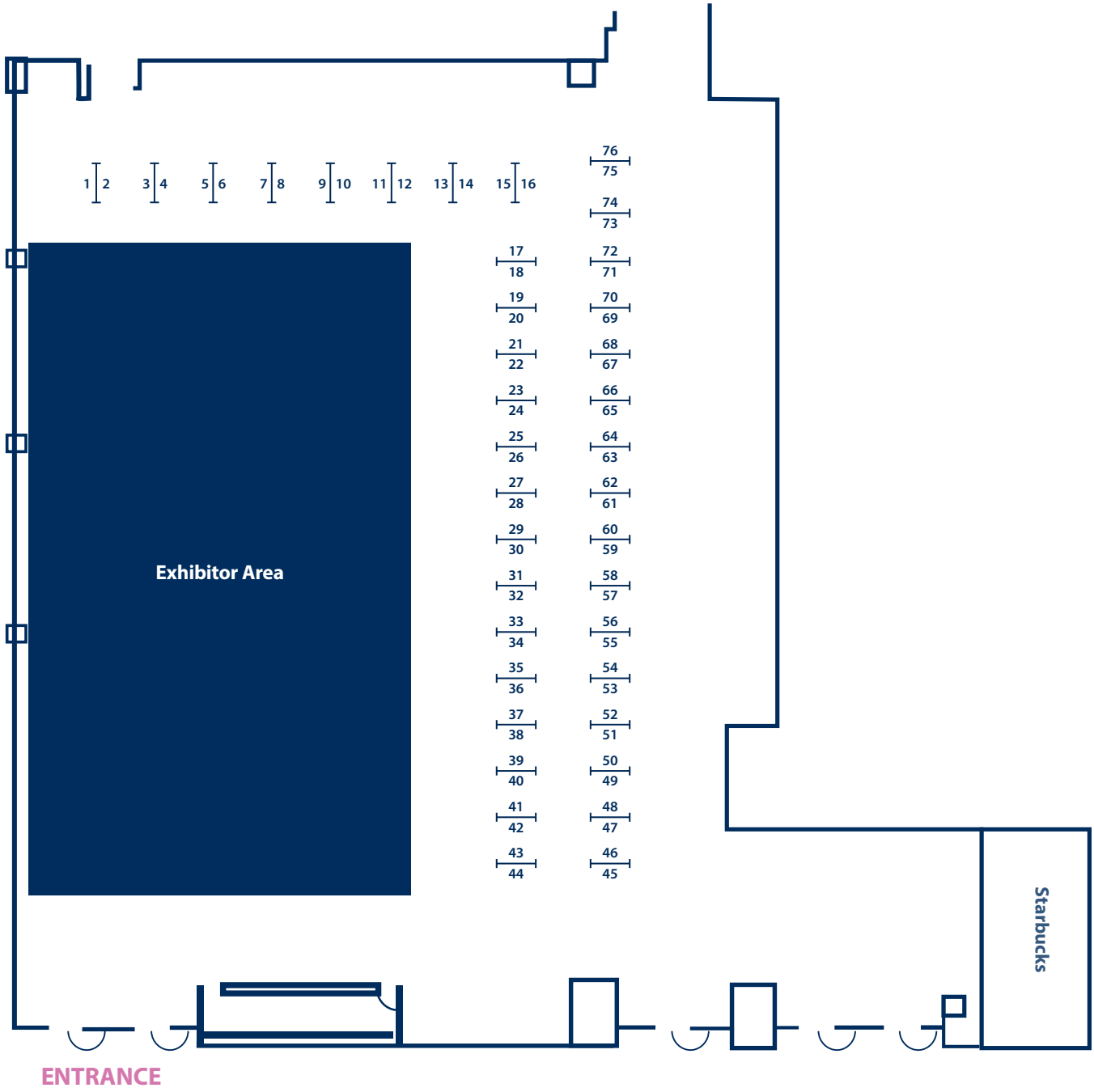

Poster Presentation Index

Poster Categories

01 **Interleukin-27 Acts on Macrophages to Tune Colon Epithelial Function**

Caroline Andrews[1], Wenqing Li[1], Julie Hixon[1], Maggie Cam[2], Scott Durum[1]. *[1]National Institutes of Health, Frederick, MD, USA. [2]National Institutes of Health, Bethesda, MD, USA.*

02 **Histological Characterization of Testicular Development of *Apis mellifera* Drones During Sexual Maturation**

Colby Klein, Sophie Derveau, Ivanna Kozii, Sarah Wood, Roman Koziy, Ihor Dvylyuk, Elemir Simko. *Western College of Veterinary Medicine, University of Saskatchewan, Saskatoon, SK, Canada.*

03 **Historical Histological Background Findings at Intramuscular Injection Sites in Control Rabbits**

Elizabeth Goldsmith[1], Keith Nelson[2]. *[1]Colorado State University, Fort Collins, CO, USA. [2]MPI Research, Mattawan, MI, USA.*

04 **Transcranial A2A Agonism Induces a Neuroprotective State That Resists the Damaging Effects of Mild Traumatic Brain Injury**

Kara Corps[1], Kenneth Jacobson[2], Dorian McGavern[1]. *[1]National Institute of Neurological Disorders and Stroke, Bethesda, MD, USA. [2]National Institute of Diabetes and Digestive and Kidney Diseases, Bethesda, MD, USA.*

05 **The Effects of ALK5 Inhibition on Cartilaginous Tissues of Sprague-Dawley Rats**

Ryan Schafbuch[1,2], Rebecca Saunders[3], Dan Hogan[3], Abigail Durkes[1,2]. *[1]Purdue University Department of Comparative Pathobiology, West Lafayette, IN, USA. [2]Indiana Animal Disease Diagnostic Laboratory, West Lafayette, IN, USA. [3]Purdue University Department of Veterinary Clinical Sciences, West Lafayette, IN, USA.*

06 **Generation of Canine Immortalized Leukocyte Cell Lines for Immunological Studies**

Ingrid Cornax, Victor Nizet. *University of California San Diego, La Jolla, CA, USA.*

07 **Pathology of the Blood-Tumor Barrier in Brain Metastases of Lung Cancer**

Alexandra Dieterly, Gozde Uzunalli, Chinyere Kemet, Arvin Soepriatna, Aparna Shinde, Craig Goergen, Michael Wendt, Tiffany Lyle. *Purdue University, West Lafayette, IN, USA.*

08 **The SIX1 Oncofetal Protein Mediates Endometrial Basal Cell Metaplasia following Neonatal Exposure to Diethylstilbestrol**

Alisa Suen[1], Wendy Jefferson[2], Carmen Williams[2], Charles Wood[3]. *[1]ORISE Fellow at US EPA, Durham, NC, USA. [2]NIEHS, NIH, Durham, NC, USA. [3]Office of Research and Development, US EPA, Durham, NC, USA.*

09 **Effects of Engineered *Bacillus anthracis* Toxin on Canine Osteosarcoma: *In Vitro* Studies**

Jonathan Fonseca[1], Ivone Mackowiak[1], Adriana Nishiya[1], Márcia Nagamine[1], Shihui Liu[2], Stephen Leppla[2], Jerrold Ward[3], Maria Dagli[1]. *[1]University of São Paulo, School of Veterinary Medicine and Animal Science, Laboratory of Experimental and Comparative Oncology, São Paulo, Brazil. [2]Laboratory of Parasitic Diseases, National Institute of Allergy and Infectious Diseases, National Institutes of Health, Bethesda, MD, USA. [3]Laboratory of Immunogenetics, NIAID, NIH, Bethesda, MD, USA.*

10 **Using Methylene Blue Photodynamic Reaction to Obtain Cancer Vaccines**

Murilo Del Grande, Maria Lucia Zaidan Dagli. *University of São Paulo, São Paulo, Brazil.*

11 **A Systematic Review of the Histopathologic Findings following Intraocular Recombinant Adeno-Associated Virus Vector Administration in Cynomolgus Macaques *(Macaca fascicularis)***

Annie Zimmerman[1,2], Ryan Boyd[2], Joshua Bartoe[2], Krishna Yekkala[2], Keith Nelson[2]. *[1]Michigan State University, Lansing, MI, USA. [2]MPI, Mattawan, MI, USA.*

12 **Repeated Administration of Cisplatin Increases EGFR/EGFR Activation and Renal Fibrosis in Kras4bG12D Lung Adenocarcinoma-Bearing Mice, but Kidney Injury Is Further Exacerbated with Erlotinib/Cisplatin Combination Treatment**

Cierra Sharp[1], Mark Doll[1], Tess Dupre[2], Levi Beverly[1], Leah Siskind[1]. *[1]University of Louisville, Louisville, KY, USA. [2]University of Arizona, Tucson, AZ, USA.*

13 **Systematic Investigation of Sciatic Nerve Processing Parameters**

Jessica S. Fortin[1], Elizabeth A. Chlipala[2], Daniel P. Shaw[1], Brad Bolon[3]. *[1]Veterinary Medical Diagnostic Laboratory, University of Missouri, Columbia, MO, USA. [2]Premier Laboratory (LLC), Boulder, CO, USA. [3]GEMpath Inc., Longmont, CO, USA.*

14 **The Impact of Different Assay Platforms on the Performance of Five Renal Injury Biomarker Assays for Rat Urine**

Diane Hamlin, Albert Eric Schultze. *Eli Lilly and Company, Indianapolis, IN, USA.*

15 **Localization of Biomarkers in Murine Polycystic Kidney Disease by Tissue Mass Spectrometry Imaging**

Dinesh Bangari, Cristina Silvescu, Laurie Smith, Lilu Guo, Mandy Cromwell, Sue Ryan, Petra Oliva, Alla Klos, Thomas O'Shea, Oxana Beskrovnaya, Beth Thurberg, Walter Korfmacher, Thomas Natoli. *Sanofi, Framingham, MA, USA.*

16 Elevation of Urinary MCP-1 in Patients with Acute Kidney Injury Receiving Lung Cancer Chemotherapy

Hiroyuki Watanabe, Mio Fukuda, Satohiro Masuda. *Department of Pharmacy, Kyushu University Hospital, Fukuoka, Japan.*

17 A Mouse Model of Immune-Complex Mediated Vascular Disease

Lykke Boysen[1,2], Lone H. Landsy[3], Birgitte M. Viuff[1], Jens Lykkesfeldt[2], Brian Lauritzen[1]. *[1]Toxicology, Safety Pharmacology and Toxicopathology, Non-clinical Development, Novo Nordisk A/S, Måløv, Denmark. [2]Experimental Pharmacology and Toxicology, Faculty of Health and Medical Sciences, University of Copenhagen, Frederiksberg, Denmark. [3]Immunogenicity Assessment, Non-clinical Development, Novo Nordisk A/S, Måløv, Denmark.*

18 Validation of Flow Cytometry-Based Quantitation of Reticulated Platelets in Cynomolgus Monkeys and Wistar Rats

Madhu Sirivelu[1], Deborah Carraher[1], Kim Lewis[1], James Warneke[1], Rodrigo Laureano[1], William Reagan[2], Laurence Whiteley[1]. *[1]Pfizer, Inc., Andover, MA, USA. [2]Pfizer, Inc., Groton, CT, USA.*

19 Evaluation of the Flavonoid Antioxidants, *alpha*-Glycosyl Isoquercitrin and Isoquercetrin, for Genotoxic Potential

Cheryl Hobbs[1], Mihoko Koyanagi[2], Carol Swartz[1], Jeffrey Davis[1], Sawako Kasamoto[3], Robert Maronpot[4], Leslie Recio[1], Shim-mo Hayashi[2]. *[1]Integrated Laboratory Systems, Inc., Research Triangle Park, NC, USA. [2]San-Ei Gen F.F.I., Inc., Osaka, Japan. [3]Public Interest Incorporated Foundation Biosafety Research Center, Shizuoka, Japan. [4]Maronpot Consulting LLC, Raleigh, NC, USA.*

20 Histomorphologic Patterns of Toxicity Associated with Seven Renal Toxicants in NHP and Their Urinary Biomarker Correlates

Sean Troth[1], Katerina Vlasakova[1], Yi-Zhong Gu[1], Jarig Darbes[2], Flavia Pasello dos Santos[2], Takayuki Tsuchiya[1], Robert Peiffer[1], Frank Sistare[1], Warren Glaab[1]. *[1]Merck, West Point, PA, USA. [2]MSD, Mirabel, France.*

21 Measurement of Urea Nitrogen in Broncho-Alveolar Lavage Fluids (BALF) in Nonhuman Primates (NHP)

Virginie Allegret, Luc Huard, Jeffrey McCartney, Rina Massarelli, Florence Poitout. *Charles River Laboratories, Senneville, QC, Canada.*

22 INHAND: International Harmonization of Nomenclature and Diagnostic Criteria for Lesions—An Update—2018

Charlotte Keenan[1], John Vahle[2], Dawn Goodman[3], Emily Meseck[4], Ronald Herbert[5], Alys Bradley[6], Matt Jacobsen[7], Rupert Kellner[8], Susanne Rittinghausen[8], Christine Ruehl-Fehlert[9], Thomas Nolte[10], Shim-mo Hayashi[11], Takanori Harada[12], Katsuhiko Yoshizawa[13]. *[1]CM Keenan ToxPath Consulting, Doylestown, PA, USA. [2]Eli Lilly & Company, Indianapolis, IN, USA. [3]Independent Consultant, Potomac, MD, USA. [4]Novartis Institute for Biomedical Research, East Hanover, NJ, USA. [5]NIEHS, Research Triangle Park, NC, USA. [6]Charles River Laboratories, Tranent, East Lothian, United Kingdom. [7]AstraZeneca, Alderley Park Macclesfield, United Kingdom. [8]Fraunhofer ITEM, Hannover, Germany. [9]Bayer Schering Pharma AG, Wuppertal, Germany. [10]Boehringer Ingelheim Pharma GmbH & Co. KG, Biberach an der Riss, Germany. [11]San-Ei Gen F.F.I., Inc., Ikuno Osaka, Japan. [12]The Institute of Environmental Toxicology, Joso-shi, Ibaraki, Japan. [13]Mukogawa Women's University, Nishinomiya, Hyogo, Japan.*

23 Interpretation of Organ Weight Changes in a Rat Preweaning Juvenile Toxicity Study with Negative Growth Effects

Cindy Fishman[1], Lorrie Posobiec[1], Susan Laffan[1], Mark Price[2], Dinesh Stanislaus[1], Jeffrey Charlap[3], Michelle Elliott[3]. *[1]GlaxoSmithKline, King of Prussia, PA, USA. [2]GlaxoSmithKline, Ware, United Kingdom. [3]Charles River, Horsham, PA, USA.*

24 Characterization of Endometrial Stromal Polyp Subtypes in the Rat

Erin Quist[1], Daven Jackson-Humbles[2], Karen Cimon[1], Lauren Shelby[3], Mark Cesta[2], Norris Flagler[2], Gabrielle Willson[1], Ron Herbert[2], Darlene Dixon[4]. *[1]Experimental Pathology Laboratories, Inc., Durham, NC, USA. [2]Cellular and Molecular Pathology Branch, National Toxicology Program, National Institute of Environmental Health Sciences, Research Triangle Park, NC, USA. [3]College of Veterinary Medicine, Kansas State University, Manhattan, KS, USA. [4]NTP Laboratory Branch, National Toxicology Program, National Institute of Environmental Health Sciences, Research Triangle Park, NC, USA.*

25 Retrospective Analysis of Fungal Rhinitis in Sprague-Dawley Rats: A Decade of Carcinogenicity Studies

Jennifer Lamoureux[1], Karen Carlton[2], Charissa Dean[1], Keith Nelson[1]. *[1]MPI Research, Mattawan, MI, USA. [2]University of Guelph, Guelph, ON, Canada.*

26 Pathological Changes—Including Cardiovascular Changes—In Cynomolgus Monkeys Induced by Anti-CD47 Monoclonal Antibody

Ke Chen[1,2,3], Shuang Qiu[1,2], Tao Chen[1,2], Peter Mann[4], Xiaobo Cen[1,2,3]. *[1]Westchina-Frontier Pharma Tech Co., Ltd, Chengdu, China. [2]National Chengdu Center for Safety Evaluation of Drugs, Chengdu, China. [3]West China School of Medicine, West China Hospital, Sichuan University, Chengdu, China. [4]Experimental Pathology Laboratories, Inc., Seattle, WA, USA.*

27 Cathepsin K Inhibitor Associated with Minimal Change-Like Renal Changes in Rhesus Monkeys

Laura Gumprecht. *Merck & Co., Inc., West Point, PA, USA.*

28 Incidence of Atypical Wistar Rat Advia® Cytograms and the Effects on Select Hematology Parameters at Covance-Madison

Mandy Meindel, Holly Jordan, Laura Wieczorkiewicz. *Covance, Madison, WI, USA.*

29 Necrohemorrhagic Pneumonia Caused by Extraintestinal *Escherichia coli* in Multiple Research Dogs

Michelle Magagna[1], April George[2], Caitlyn Carter[2], Charissa Dean[2], Keith Nelson[2]. *[1]Michigan State University Veterinary Diagnostic Laboratory, Lansing, MI, USA. [2]MPI Research, Mattawan, MI, USA.*

30 Tube Type and Centrifugation Conditions Contribute to Hemolyzed Serum Samples in Rats

Mike Logan, Tammy Palenski, Samantha Wildeboer, Sue Riendl, Irina Skarzhin, Dimple Patel, Joslyn Lewis, Kelly Robinson, Kirstin Barnhart. *AbbVie, North Chicago, IL, USA.*

31 Spontaneous True Hermaphroditism in a Sprague-Dawley Rat

Norifumi Takimoto[1], Noriaki Ishigami[1], Kenji Nakamura[2], Atsuko Murai[2], Kengo Namiki[2], Daisuke Hibi[1], Koji Shimouchi[1]. *[1]Ono Pharmaceutical Co., Ltd., Osaka, Japan. [2]Ono Pharmaceutical Co., Ltd., Fukui, Japan.*

32 **Age-Related Changes in Hematopoietic Activity in the Bone Marrow, Spleen, and Liver in Neonatal, Juvenile, and Young/Adult Göttingen Minipigs**

Pierluigi Fant[1], Marjolein van Heerden[2]. *[1]Charles River, Lyon, France. [2]Janssen Research & Development, Beerse, Belgium.*

33 **Liver Hypertrophy and Toxicity to Microcystin-LR: Gender Differences in CD-1 Mice following Oral Administration**

Shambhunath Choudhary[1], Mark Morse[1], Christopher Weghorst[2], Thomas Knobloch[2], Igor Mrdjen[2], Randy Ruch[3], Jiyoung Lee[2]. *[1]Charles River Laboratories, Spencerville, OH, USA. [2]Ohio State University, Columbus, OH, USA. [3]University of Toledo, Toledo, OH, USA.*

34 **Nucleoside/tide Inhibitors—Mitochondrial Toxicity or Other Mechanisms?**

Sherry Morgan, Michael Liguori, Rich Peterson, Mike Logan, Meg Ramos, George Foley. *AbbVie, North Chicago, IL, USA.*

35 **Graft-vs-Host Disease (GVHD) in NSG (NOD-SCID il2rγ-/-) Mice Engrafted with Human Hematopoietic Stem Cells (HSPCs)—Preclinical Findings and Clinical Relevance**

Sundeep Chandra, Carlos Fonck, Valerie Ackley, Todd Oppeneer, Jill Woloszynek, Greg Hayes, Soumi Gupta, Charles O'Neill. *BioMarin Pharmaceutical Inc., San Rafael, CA, USA.*

36 **Relationship between Teicoplanin-Induced Toxicity and Blood Concentrations in Neonates and Children**

Takaaki Yamada, Satohiro Masuda. *Department of Pharmacy, Kyushu University Hospital, Fukuoka, Japan.*

37 **Spontaneous Hepatic Artery Degeneration/Necrosis in Young Male Sprague-Dawley Rats**

Lily Yee, Tracy Carlson. *MPI Research, Mattawan, MI, USA.*

38 **Use of Telepathology for Pathology Peer Review in Multinational Studies**

Gabe Siegel[1], Dan Regelman[1], Robert Maronpot[2], Moti Rosenstock[3], Abraham Nyska[4]. *[1]Augmentiqs, Misgav, Israel. [2]Maronpot Consulting, Raleigh, NC, USA. [3]Rosenstock Toxicologic Consulting, Haifa, Israel. [4]Tel Aviv University, Timrat, Israel.*

39 **Enabling Toxicologic Pathologists Using QuPATH, an Open Source Digital Pathology and Image Analysis Software Solution**

Daniel Rudmann[1], Abigail Godbold[1], Maureen O'Brien[2], Brent Walling[1]. *[1]Charles River Laboratories, Ashland, OH, USA. [2]Charles River Laboratories, Frederick, MD, USA.*

40 **Multiplexing Tyrosine Hydroxylase Immunohistochemistry and Luxol Fast Blue-Hematoxylin for Neuroanatomical Differentiation Using Stereology**

Michael Staup, Danielle Brown, David Weil, Na Li, Jane Goad, Cynthia Swanson, Kyle Takayama. *Charles River Laboratories, Durham, NC, USA.*

41 **Quantitative versus Semiquantitative Assessment of Fibrosis in Unilateral Ureter Obstruction (UUO) Model in Mice**

Jing Ying Ma[1], Bindu Bennet[2], Vinicius Carreira[1]. *[1]Pathology and Toxicology, Janssen Research & Development, LLC, San Diego, CA, USA. [2]Pathology and Toxicology, Janssen Research & Development, LLC, Spring House, PA., USA.*

42 **Glomerular Identification and Quantification of Histological Phenotypes in the Mouse Using Image Analysis and Machine Learning**

Susan Sheehan, Ron Korstanje. *The Jackson Laboratory, Bar Harbor, ME, USA.*

43 **Artificial Intelligence (AI)-Based Image Analysis and Decision Support System (iADSS) to Aid Pathologists in Analysis and Classification of Histopathology Images of WISTAR Rat Kidneys**

Tijo Thomas, Uttara Joshi, Anindya Hajra. *Aditya Imaging Information Technologies, Thane West, India.*

44 **A Robust *In Vivo* Model of Brain Metastases of Lung Cancer**

Gozde Uzunalli, Alexandra Dieterly, Chinyere Kemet, Arvin Soepriatna, Aparna Shinde, Craig Goergen, Michael Wendt, L. Tiffany Lyle. *Purdue University, West Lafayette, IN, USA.*

45 **Establishment of an *In Vitro* Hepatocarcinogenesis Model: Cell Proliferation of AML12 Cell Line Cultured in Presence of NNK**

Andrea Midory Miyake, Marcia Kazumi Nagamine, Murilo Penteado Del-Grande, Nicolle Gilda de Queiroz Hazarbassanov, Cristina de Oliveira Massoco de Salles Gomes, Ivone Izabel Mackowiak da Fonseca, Maria Lucia Zaidan Dagli. *Universidade de São Paulo, São Paulo, Brazil.*

46 **Toxicogenomics Study of Pentabrominated Diphenyl Ethers (DE-71 Mixture and Its Congener PBDE-47) in Rat Liver after Early Life Exposure**

Arun Pandiri[1], Keith Shockley[1], Dan Morgan[1], Grace Kissling[1], Thai-Vu Ton[1], Ralph Wilson[1], Sukhdev Brar[1], Amy Brix[2], June Dunnick[1]. *[1]National Institute of Environmental Health Sciences, Research Triangle Park, NC, USA. [2]Experimental Pathology Laboratories, Inc, Research Triangle Park, NC, USA.*

47 **Fibrosarcoma with Unique Histomorphologic Features in the Small Intestine of Wistar Han Rats in a Two-Year Carcinogenicity Study**

Kiran Palyada, Thomas Forest, Christine Reichard, Caron Leach, Takayuki Tsuchiya. *Merck and Company, West Point, PA, USA.*

48 **Mitochondrial Genomic Alterations in Spontaneous and Chemical-Induced Hepatocellular Carcinomas in B6C3F1/N Mice**

Miaofei Xu[1], Adam Burkholder[2], David Fargo[3], Jacqui Marzec[4], Steven Kleeberger[4], Gregory Solomon[5], Robert Sills[1], Arun Pandiri[1]. *[1]Division of National Toxicology Program (DNTP), NIEHS, Research Triangle Park, NC, USA. [2]Center for Integrative Bioinformatics, NIEHS, Research Triangle Park, NC, USA. [3]Center for Integrative Bioinformatics, NIEHS, Research Triangle Park, NC, USA. [4]Immunity, Inflammation, and Diseases Laboratory, NIEHS, Research Triangle Park, NC, USA. [5]Epigenemoic Core, NIEHS, Research Triangle Park, NC, USA.*

49 Preclinical Activity of Tipifarnib in Cutaneous T-Cell Lymphoma

Rebecca Kohnken[1], Betina McNeil[1], Jing Wen[1], Kathleen McConnell[1], Basem William[1], Francis Burrows[2], Pierluigi Porcu[3], Anjali Mishra[1]. [1]*Ohio State University, Columbus, OH, USA.* [2]*Kura Oncology, San Diego, CA, USA.* [3]*Thomas Jefferson University, Philadelphia, PA, USA.*

50 Toxicity and Toxicokinetic Study of Subcutaneously Administered RPh201 in Minipigs

Yuval Ramot[1], Zadik Hazan[2], Andre Lucassen[2], Konstantin Adamsky[2], Vanessa Ross[3], Nigel Young[3], Abraham Nyska[4]. [1]*Hadadssah- Hebrew University Medical Center, Jerusalem, Israel.* [2]*Regenera Pharma, Nes-Ziona, Israel.* [3]*Envigo, Ltd., Alconbury, Cambridgeshire, United Kingdom.* [4]*Consultant in Toxicologic Pathology, Timrat, Israel.*

51 Inhaled Furan Selectively Damages Club Cells in Lungs of A/J Mice

Alexandru-Flaviu Tabaran[1,2], Lisa A. Peterson[3], M. Gerard O'Sullivan[1,2]. [1]*College of Veterinary Medicine, University of Minnesota, Saint Paul, MN, USA.* [2]*Comparative Pathology Shared Resource, Masonic Cancer Center, University of Minnesota, Saint Paul, MN, USA.* [3]*Division of Environmental Health Sciences, Masonic Cancer Center, University of Minnesota, Minneapolis, MN, USA.*

52 Infusion Procedure-Related Pathology of Intravenous Catheterized Rats

Amit Kumar[1,2], David Rehagen[2]. [1]*Michigan State University, Lansing, MI, USA.* [2]*MPI Research, Mattawan, MI, USA.*

53 Characterization of a Novel Pulmonary Arteriopathy in Control Beagle Dogs

Juliane Daggett[1], Keith Nelson[2], James Reindel[2]. [1]*Midwestern University, College of Veterinary Medicine, Glendale, AZ, USA.* [2]*MPI Research, Mattawan, MI, USA.*

54 Proposed Mode of Action for Uterine Adenocarcinomas in Han Wistar Rats Treated with Isopyrazam (IZM)

Jayne Wright[1], Elizabeth McInnes[2], Sue Yi[2], Richard Peffer[3], David Cowie[2], Paul Parsons[4], Richard Currie[2], Ryan Richards-Doran[2], Douglas Wolf[3], Kristin Lichti-Kaiser[3]. [1]*Syngenta Consultant, Bracknell, United Kingdom.* [2]*Syngenta, Bracknell, United Kingdom.* [3]*Syngenta, Greensboro, NC, USA.* [4]*Exponent, Liverpool, United Kingdom.*

55 An Immunohistochemical Investigation of TGFß Receptor-1 Inhibitor-Induced Renal Epithelial Proliferative Lesions in Cynomolgus Monkeys

Jing Ying Ma, Sandra Snook, Vinicius Carreira. *Preclinical Development & Safety, Janssen Research & Development, LLC, San Diego, CA, USA.*

56 GPER-Dependent Transactivation of EGFR Is Required for Human Leiomyoma Cell Proliferation Induced by Cadmium (Cd): A Nongenomic Mechanism for Cd's "Metalloestrogenic" Effects

Jingli Liu, Linda Yu, Lysandra Castro, Yitang Yan, Alanna Burwell, Darlene Dixon. *Molecular Pathogenesis Group, National Toxicology Program (NTP) Laboratory, National Institute of Environmental Health Sciences, National Institutes of Health, Research Triangle Park, NC, USA.*

57 Pancreatic Effects of Valosin-Containing Protein (VCP) Inhibition in Mice and Rats

Karyn Enos, Francis Wolenski, James Gavin, Sean Harrison, Allison Berger, Sandy Gould, William Mallender. *Takeda Pharmaceuticals International Co., Cambridge, MA, USA.*

58 Renal Lesions Associated with Soy-Deficient Diet in Rats

Catherine Picut[1], Eli Parker[1], Stephanie White-Hunt[1], Kathleen Szabo[2], Jessica Keen[3], Pragati Coder[3], Pallavi McElroy[3].[1]Charles River Laboratories, Durham, NC, USA. [2]*Charles River Laboratories, Frederick, MD, USA.* [3]*Charles River Laboratories, Ashland, OH, USA.*

59 Histologic Background Findings of the Lung in Beagle Dogs: A Comparison between Apical and Diaphragmatic Lobes

Juliane Daggett[1], James Reindel[2], Keith Nelson[2]. [1]*Midwestern University, College of Veterinary Medicine, Glendale, AZ, USA.* [2]*MPI Research, Mattawan, MI, USA.*

60 Effect of Combined Dyslipidemia and Hyperglycemia on Diabetic Peripheral Neuropathy in Alloxan-Induced Diabetic WBN/Kob Rats

Kiyokazu Ozaki, Tetsuro Matsuura. *Setsunan University, Osaka, Japan.*

61 Glomerulosclerosis and Dysplasia of Medulla, Gentamicin-Induced Unique Nephrotoxicity in Juvenile Rats

Kiyonori Kai, Kumi Honda, Kyohei Yasuno, Shinobu Hakamata, Kazunori Fujimoto, Noriyo Niino, Kazuhiko Mori. *Daiichi Sankyo Co., Ltd., Tokyo, Japan.*

62 Adverse Effect of Intra-Arterial Carboplatin Chemotherapy for Retinoblastoma in a Rabbit Model

Lauren Himmel, Tai Oatess, Kelli Boyd, Anthony B. *Daniels. Vanderbilt University Medical Center, Nashville, TN, USA.*

63 Dapagliflozin Does Not Act as a Tumor Promoter or Progressor in a Rodent Model of Urothelial Bladder Cancer

Magnus Söderberg[1], Agathe Bédard[2], Solomon Haile[2], Bassem Attalla[2], Jason Kirk[3], Martin Billger[4]. [1]*Pathology, Drug Safety and Metabolism, IMED Biotech Unit, AstraZeneca, Gothenburg, Sweden.* [2]*Charles River Laboratories, Montréal, QC, Canada.* [3]*Regulatory Safety, Drug Safety and Metabolism, IMED Biotech Unit, AstraZeneca, Cambridge, United Kingdom.* [4]*Regulatory Safety, Drug Safety and Metabolism, IMED Biotech Unit, AstraZeneca, Gothenburg, Sweden.*

64 Step Sectioning Protocol for Comprehensive Evaluation of Cardiac Valves When Using a Mouse Model

Maureen O'Brien, Elaine Edmonds, Lauren Kuhn, Robert Jacoby. *Charles River Laboratories, Frederick, MD, USA.*

65 Novel Off-Target Effect on Urine Concentrating Ability in an Exploratory Rat Toxicity Study

Bruce LeRoy, Michael Foley, Michael Logan. *AbbVie, North Chicago, IL, USA.*

66 **Toxicity of Secondhand Tobacco Smoke on Immune Functions of Alveolar Macrophages in Mice**

Minoru Takeuchi[1], Maiko Takasaki[1], Naoko Miwa[1], Yuriko Hirono[1], Yoshiko Tanaka[1], Kent Pinkerton[2]. *[1]Kyoto Sangyo University, Kyoto, Japan. [2]UCD, Davis, CA, USA.*

67 **Evaluation of the Göttingen Minipig as a Large Animal Model for Otologic Research**

Pankaj Kumar[1], Aaron Sargeant[1], Bridget Lewis[1], Jean-Francois Lafond[2]. *[1]Charles River Labs, Spencerville, OH, USA. [2]Charles River Labs, Montréal, QC, Canada.*

68 **Anatomy, Histology and Spontaneous and Induced Pathology of the Kidney, and Selected Renal Biomarkers Reference Ranges in the Laboratory Nonhuman Primate**

Ronnie Chamanza[1], Stuart Naylor[2], Chidozie Amuzie[3], Vinicius Carreira[4], Jing Ying Ma[4], Alys Bradley[2], Brad Blankenship[5], Kevin McDorman[6], Calvert Louden[3]. *[1]Janssen Pharmaceutical Companies of Johnson & Johnson, Beerse, Belgium. [2]Charles River Laboratories, Edinburgh, United Kingdom. [3]Janssen Pharmaceutical Companies of Johnson & Johnson, Spring House, PA, USA. [4]Janssen Pharmaceutical Companies of Johnson & Johnson, La Jolla, CA, USA. [5]Charles River Laboratories, Reno, NV, USA. [6]Charles River Laboratories, Wilmington, MA, USA.*

69 **It's Not Just a Rat Phenomenon: A Case Example of Canine-Specific Thyroid and Pituitary Hypertrophy Secondary to UGT Induction and Increased Thyroid Hormone Metabolism**

Sandra De Jonghe[1], Ronnie Chamanza[1], Petra Vinken[1], Geert Mannens[1], Heng-Keang Lim[2], Monicah Otieno[2], Junguo Zhou[3], Gary Eichenbaum[4]. *[1]Janssen Research and Development, Beerse, Belgium. [2]Janssen Research and Development, Spring House, PA, USA. [3]Janssen Research and Development, Raritan, NJ, USA. [4]Johnson & Johnson, New Brunswick, NJ, USA.*

70 **Spice/K2-Induced Encephalopathy and Acute Renal Failure**

Eric Chang, Shaheen Fatima, Amina Farooq, Anam Umar, Ifedolapo Odebunmi, Taiwo Ajose, Chinedu Ivonye. *Morehouse School of Medicine, Atlanta, GA, USA.*

71 **Histology Atlas of the Developing Mouse Urinary Tract**

Sanam L. Kavari[1], Koichi Yabe[2], Mark J. Hoenerhoff[3], John C. Seely[4], Beth Mahler[4], Susan A. Elmore[1]. *[1]NTP, NIEHS, Cellular and Molecular Pathology Branch and National Toxicology Program, Research Triangle Park, NC, USA. [2]Medicinal Safety Research Laboratories, Kitakasai, Daiichi Sankyo Co., Ltd., Edogawa-ku, Tokyo, Japan.* [3]In Vivo *Animal Core, Unit for Laboratory Animal Medicine, University of Michigan, Ann Arbor, MI, USA. [4]Experimental Pathology Laboratories, Inc., Research Triangle Park, NC, USA.*

72 **Anti-Fibrotic Role of miR-214 in Chemically Induced Liver Cirrhosis in Rats**

Takeshi Izawa, Takashi Horiuchi, Machi Atarashi, Mitsuru Kuwamura, Jyoji Yamate. *Veterinary Pathology, Osaka Prefecture University, Izumisano, Japan.*

73 **Modulation of Hepatic Nuclear Receptors in the Progression of Non-Alcoholic Fatty Liver Disease**

Xilin Li, Zemin Wang, James Klaunig. *Indiana University, Bloomington, IN, USA.*

74 **Analysis of Hemorrhagic Diathesis in Rats Fed a High-Iron Diet**

Yohei Inai[1], Takashi Izawa[1], Mutsuki Mori[1], Machi Atarashi[1], Seiichirou Tsuchiya[2], Mitsuru Kuwamura[1], Jyoji Yamate[1]. *[1]Veterinary Pathology, Osaka Prefecture University, Osaka, Japan. [2]Sysmex Corporation, Kobe, Japan.*

Abstracts

01

Interleukin-27 Acts on Macrophages to Tune Colon Epithelial Function

Caroline Andrews[1], Wenqing Li[1], Julie Hixon[1], Maggie Cam[2], Scott Durum[1].
[1]*National Institutes of Health, Frederick, MD, USA.* [2]*National Institutes of Health, Bethesda, MD, USA.*

Introduction: Interleukin(IL)-27 administration has reduced inflammation and improved survival in murine models of inflammatory bowel disease. Conversely, genetic ablation of the IL-27 receptor demonstrated a deleterious effect of IL-27 in murine colitis. Therefore, characterization of action of IL-27 in the intestine is crucial before IL-27 can be explored as a therapy for intestinal disease.

Experimental Design: Macrophages were harvested from C57BL/6NCrl mice +/- culture with interferon-gamma and endotoxin to activate a pro-inflammatory phenotype. Macrophages were cultured alone or co-cultured with epithelial organoids derived from C57BL/6NCrl colon crypts. Cultures were stimulated for 24 hours with IL-27.

Methods: IL-27 signaling was assessed by western blot for pSTAT1. Transcriptional changes were characterized by RNA sequencing. Sequencing data was validated by real-time RT-qPCR, and secreted proteins were detected by Mesoscale immunoassay.

Results: In macrophages, IL-27 induced pSTAT1, increased *IFNG* and *NOS2* expression, and increased secretion of interferon-gamma, TNF-alpha, and IL-6. Co-culture of organoids with macrophages and IL-27 induced pSTAT1 in organoids, but IL-27 alone had no effect. RNA sequencing of colon organoids co-cultured with IL-27-stimulated macrophages detected increased expression of gene pathways crucial for pathogen responses.

Conclusion: While IL-27 had no direct effect on the colon epithelium, it induced the production of macrophage-derived soluble mediators that modulated colon epithelial function.

Impact Statement: These data elucidate a novel role for IL-27 in macrophage function and provide guidance regarding its therapeutic potential in intestinal disease.

02

Histological Characterization of Testicular Development of *Apis Mellifera* Drones During Sexual Maturation

Colby Klein, Sophie Derveau, Ivanna Kozii, Sarah Wood, Roman Koziy, Ihor Dvylyuk, Elemir Simko
Western College of Veterinary Medicine, University of Saskatchewan, Saskatoon, SK, Canada.

Background: Current risk assessment procedures for pollinator exposure to pesticides are not adequately predicting detrimental interactions reported in scientific literature. The "gold standard" for compound risk-assessment in mammals relies on histopathology which isn't employed in honey bees.

Objective: To characterize normal morphological changes of honey bee drone testes during the sexual maturation period to establish a normal benchmark for future gonadotoxicity studies.

Methods: At emergence, drones were marked and sampled daily during the sexual maturation period (2 weeks). The reproductive tract of each drone was dissected, photographed and analyzed macroscopically and microscopically.

Results: Drones undergo sexual maturation 2 weeks post emergence. Mature sperm moves from testes to seminal vesicles via vas deferens, while the testes undergo involution and atrophy. Testicular changes during sexual maturation are characterized by phases: 1) Spermatogenesis continues up to day 3; 2) By day 8, sperm have moved from testes to vas deference and seminal vesicles; 3) Testicular parenchyma degenerates with parenchymal loss by day 11 - 15; 4) Testes of matured drones consist of collapsed supporting stroma, brown pigment and tracheal network. Drone maturation and testicular involution accelerated by approximately 4 days during warmer months.

Conclusions: The testicular involution occurs in a stepwise process during sexual maturation of honey bee drones. The length of this process is influenced by environmental temperature and ranges from 9 to 14 days.

Impact Statement: This study will allow us to build towards our greater goal of developing a normal histological library to investigate gonadotoxicity of pesticides on the honey bee.

03

Historical Histological Background Findings at Intramuscular Injection Sites in Control Rabbits

Elizabeth Goldsmith[1], Keith Nelson[2].
[1]*Colorado State University, Fort Collins, CO, USA.* [2]*MPI Research, Mattawan, MI, USA.*

Introduction: Intramuscular injection sites are commonly used for vaccine safety studies, with rabbits a common large animal model. Accurate recognition and quantification of injection-related lesions in animal models improves identification of compound-related findings. The purpose of this study was to review and analyze background histological findings occurring over 10 years in control rabbits used in intramuscular injection studies.

Experimental Design: We retrospectively analyzed findings in control rabbits from multiple intramuscular injection studies conducted at MPI Research between 2007 and 2016.

Methods: Histologic lesion data were tabulated for 381 rabbits, totaling 1215 injection sites from 15 intramuscular injection studies. Comparisons of lesion prevalence were made across a range of excipients, including saline and dextrose, and adjuvants, such as GLA-SE, PHAD, aluminum hydroxide (Alum™), and DPPC.

Results: The most common findings were chronic inflammation within muscle and subcutis and myofiber degeneration in muscle. Granulomatous inflammation in the muscle was identified in animals injected with saline, GLA-SE, and PHAD. Alum™-dosed injection sites had foamy macrophages and foreign material present.

Conclusions: There are a range of histological changes associated with intramuscular injection of excipients or adjuvants, which may affect analysis of compound-related effects. Findings at injection sites vary widely between adjuvants and tissue subcompartments.

Impact Statement: This study provides an extensive review of intramuscular injection-related findings in control rabbits at a large preclinical CRO. Consideration of excipient- or adjuvant-related findings as well as those induced by the injection procedure should be a key component of any intramuscular injection study.

04

Transcranial A2A Agonism Induces a Neuroprotective State That Resists the Damaging Effects of Mild Traumatic Brain Injury

Kara Corps[1], Kenneth Jacobson[2], Dorian McGavern[1].
[1]*National Institute of Neurological Disorders and Stroke, Bethesda, MD, USA.* [2]*National Institute of Diabetes and Digestive and Kidney Diseases, Bethesda, MD, USA.*

Introduction: Traumatic brain injuries (TBI) frequently result in acute and chronic neurological consequences that affect quality of life. The failure thus far to develop efficacious therapies necessitates further investigation of pathogenic mechanisms following TBI. The mechanism(s) by which adenosine signaling modulates TBI pathogenesis is currently unknown. Studies suggest that this pathway can be targeted to improve CNS injury outcomes.

Experimental Design: We utilized our mouse model of closed-skull, compressive focal mTBI to explore the effects of transcranially promoting or blocking adenosine receptor signaling on neocortical cell death.

Materials and Methods: Age-matched C57Bl/6J mice were randomly assigned to vehicle or compound groups, anesthetized, and subjected to mTBI. Compounds were incubated transcranially for 8 hours followed by transcranial incubation of propidium iodide (PI) to label dead cells *in vivo*. Brains were collected for frozen histopathology, and PI+ dead cells were quantified following confocal imaging of coronal sections through the mTBI center.

Results: We found that A2A receptor agonists were neuroprotective following mTBI by acting in a receptor subtype-specific manner on brain-resident rather than infiltrating cells. Agonists protected the CNS parenchyma but not the meninges and were able to do so by signaling through protein kinase C δ/ε and controlling cellular pH via modulation of carbonic anhydrase IX.

Conclusion: A2A agonists induce a neuroprotective state that resists parenchymal damage due to mTBI.

Impact Statement: We describe amelioration of acute cell death following mTBI by transcranial application of A2A agonists, warranting further evaluation of the clinical potential of such compounds.

05

The Effects of ALK5 Inhibition on Cartilaginous Tissues of Sprague-Dawley Rats

Ryan Schafbuch[1,2], Rebecca Saunders[3], Dan Hogan[3], Abigail Durkes[1,2].
[1]*Purdue University Department of Comparative Pathobiology, West Lafayette, IN, USA.* [2]*Indiana Animal Disease Diagnostic Laboratory, West Lafayette, IN, USA.* [3]*Purdue University Department of Veterinary Clinical Sciences, West Lafayette, IN, USA.*

Introduction/Objectives: Signaling through the TGF-β1 receptor, ALK5, is important in the development and function of multiple connective tissues, including heart valves, cartilage, tendon, and bone. ALK5 inhibition is involved in the pathogenesis of myxomatous mitral valve degeneration in rats. Our objective was to determine if ALK5 inhibition could induce degenerative changes in articular cartilage, physes, or intervertebral discs, which share many common regulatory pathways with heart valves.

Experimental Design: Ten Sprague-Dawley rats were randomly divided into 2 treatment groups: 5 negative control and 5 ALK5 inhibitor. Two pathologists, blinded to treatment group, individually analyzed tissues.

Methods: Control rats received 30 mg/kg vehicle (0.5% HPMC, PBS, 0.1 N HCl), and ALK5 inhibitor rats received 100 mg/kg LY2109761 (an Alk5 antagonist) by oral gavage once daily for 14 days. Sections of intervertebral discs and distal femurs were processed for microscopic evaluation and were scanned to Aperio for digital evaluation.

Results: Physeal clefting with infractions of primary spongiosa was observed in ALK5 inhibitor rats but not control rats. Physeal thickness did not differ significantly between treatment groups. There were no histologic differences in the articular cartilage or intervertebral discs between the two treatment groups.

Conclusion: ALK5 inhibition was associated with physeal clefting and infractions of the distal femoral physis, but no degenerative changes in articular cartilage or intervertebral discs were observed in Sprague-Dawley rats.

Impact Statement: Further studies are warranted, but these data suggest signaling pathways involved in osteochondral disorders may be functionally related to mitral valve disease.

06

Generation of Canine Immortalized Leukocyte Cell Lines for Immunological Studies

Ingrid Cornax, Victor Nizet.
University of California San Diego, La Jolla, CA, USA.

Introduction: Dogs are an intriguing model for the study of complex heritable traits affecting immune function. Two hundred years of intensive breeding has resulted in purebred dogs that express unique phenotypes that manifest in differential susceptibility to infectious, inflammatory, and immune-mediated diseases. Unfortunately, the canine immune system is understudied and poorly understood due to a lack of essential reagents. The only currently available canine "macrophage-like" immortalized cell-line (DH82) exhibits a minimal to absent response to key inflammatory stimuli and is therefore of minimal relevance to studies of immune function.

Methods: To address the need for better canine leukocyte cell lines, we are developing a standardized retroviral delivery protocol to generate conditionally immortalized myeloid progenitors that can be terminally differentiated into neutrophils, macrophages, and dendritic cells.

Results: In initial experiments, macrophages derived from this system produced the key pro-inflammatory cytokine IL-1β in response to lipopolysaccharide and ATP at levels comparable to those of stimulated primary bone marrow-derived macrophages. Further analysis is underway to evaluate antimicrobial activity, phagocytosis, reactive oxygen species generation, and cytokine production of these cells.

Conclusion: Once established, this immortalization method will be used to generate cell lines from a variety of representative dog breeds and enable systematic *in vitro* testing of breed-specific leukocyte function.

Impact Statement: Determining how genetic background affects leukocyte activity could aid in the development of novel therapeutics customized to an individual dog's immunophenotype.

07

Pathology of the Blood-Tumor Barrier in Brain Metastases of Lung Cancer

Alexandra Dieterly, Gozde Uzunalli, Chinyere Kemet, Arvin Soepriatna, Aparna Shinde, Craig Goergen, Michael Wendt, Tiffany Lyle.
Purdue University, West Lafayette, IN, USA.

Introduction: The incidence of brain metastases of lung cancer, particularly non-small cell lung cancer (NSCLC), is increasing. Treatment of these metastases is challenging due to the shift of the blood-brain barrier (BBB) to the blood-tumor barrier (BTB). We aim to identify structural alterations of the BTB in NSCLC brain metastases, which may serve as druggable targets.

Experimental Design: We hypothesized a distinct difference in pathology is present in the BTB compared to the BBB in NSCLC brain metastases. An experimental model was developed using intracardiac injection of brain-seeking cells in athymic nude mice (n=36). Functional components of the BBB and BTB were analyzed qualitatively and quantitatively using immunofluorescence microscopy. Area of antibody expression was analyzed from 5 brain metastases (BTB) and 5 unaffected regions (BBB).

Results: Immunofluorescence analysis revealed a 5.4-fold decrease in CD31 expression ($p<0.0001$) and a 1.7-fold decrease in the tight junction adapter protein ZO-1 ($p<0.0001$). A 2.5 decrease in PDGFR-β ($p<0.0001$), a pan-pericyte marker, and a 2-fold decrease in desmin+ pericytes ($p<0.01$) were present in the BTB. Basement membrane proteins, collagen-IV and laminin-α2, were decreased 1.7-fold ($p<0.0001$) and 7.4-fold ($p<0.0001$), respectively, in the BTB. Increased GFAP+ astrocytes were present surrounding brain metastases.

Conclusion: Our results demonstrate a loss of microvasculature, tight junctions, basement membranes, and pericytes in the BTB compared to the BBB in NSCLC brain metastases.

Translational Impact: Identified BTB alterations may serve as therapeutic targets for treatment of NSCLC brain metastases and improve patient survival.

08

The SIX1 Oncofetal Protein Mediates Endometrial Basal Cell Metaplasia following Neonatal Exposure to Diethylstilbestrol

Alisa Suen[1], Wendy Jefferson[2], Carmen Williams[2], Charles Wood[3].
[1]*ORISE Fellow at US EPA, Durham, NC, USA.* [2]*NIEHS, NIH, Durham, NC, USA.*
[3]*Office of Research and Development, US EPA, Durham, NC, USA.*

Early-life exposure to estrogenic chemicals can increase cancer risk, potentially by disrupting normal patterns of cellular differentiation. In a model of this effect, female mice exposed on postnatal day 1–5 to diethylstilbestrol (DES) develop endometrial adenocarcinoma as adults. Neoplastic glands are composed of abnormal populations of basal cells (cytokeratin [CK]14+), luminal cells (CK18+), and low numbers of "mixed" basal/luminal cells (CK14/18+), all of which express the oncofetal protein sine oculis homeobox 1 (SIX1). We hypothesized that SIX1 is necessary for DES-induced differentiation patterns and carcinogenesis. To test this hypothesis, a conditional knockout model was generated in which floxed *Six1* was excised in the uterus using PgR-cre. The most prominent change in DES-exposed SIX1 knockout (DES-*Six1*d/d) mice was the absence of basal cells in the uterine horns. Quantitative image analysis indicated a >10-fold decrease in CK14 labeling in the uterine horns of DES-*Six1* d/d mice compared to DES-exposed SIX1 wildtype (DES-*Six1*+/+) mice. However, DES-*Six1*d/d mice exhibited a 38% increase in cancer incidence compared to DES-*Six1*+/+ mice (7/9 DES-*Six1*d/d vs. 4/10 DES-*Six1*+/+) at 6 months old. Interestingly, mixed cells were still present in DES-*Six1*d/d mice. These findings demonstrate that SIX1 is a cellular differentiation factor necessary for DES-induced basal cells but not mixed cells or cancer. These data also suggest that mixed cells are cancer progenitor cells and that SIX1 decreases uterine carcinogenesis by facilitating basal differentiation. This abstract does not reflect US EPA policy.

09

Effects of Engineered *Bacillus anthracis* Toxin on Canine Osteosarcoma: *In Vitro* Studies

Jonathan Fonseca[1], Ivone Mackowiak[1], Adriana Nishiya[1], Márcia Nagamine[1], Shihui Liu[2], Stephen Leppla[2], Jerrold Ward[3], Maria Dagli[1].
[1]*University of São Paulo, School of Veterinary Medicine and Animal Science, Laboratory of Experimental and Comparative Oncology, São Paulo, Brazil.* [2]*Laboratory of Parasitic Diseases, National Institute of Allergy and Infectious Diseases, National Institutes of Health, Bethesda, MD, USA.* [3]*Laboratory of Immunogenetics, NIAID, NIH, Bethesda, MD, USA.*

Introduction: Osteosarcomas are one of the most common malignancies in dogs. The uPAs and MMPs are proteases overexpressed in several neoplastic cells but rarely present in normal cells. A *Bacillus anthracis* toxin was reengineered to be activated by uPA and/or MMPs, acting selectively on neoplastic cells.

Experimental design: The toxins PA, PAL1, PAU2, and FP59 (a modified version LF with higher toxicity than LF), were tested on canine (D17) and human (MG63) osteosarcoma cell lines and in primary canine osteosarcoma cells (CL3).

Methods: Cell density was evaluated by MTT and apoptosis was quantified with fluorescence microscopy by staining with Acridine Orange associated with Ethidium Bromide.

Results: Our results of optical density showed that in three cell lines the toxins were effective to provoke cell death, mostly with FP59 in comparison to LF (MG63 – 0.246 for control, 0.074 for LF and 0.010 for FP59; CL3 – 0.228 for control, 0.104 for LF and 0.014 for FP59; D17 - 0.236 for control, 0.225 for LF and 0.021 for FP59), as expected. We observed higher rates of apoptosis with FP59 when compared to control (CL3 – 22,74% vs 4,5% for control; MG63 – 33,33% for FP59 vs 2,0% for control).

Conclusion: We concluded that the reengineered *Bacillus anthracis* toxin was effective to provoke cell death in canine and human osteosarcoma.

Impact Statement: Based upon our evaluation, the re-engineered *Bacillus anthracis* toxin it is a potential drug therapy for the treatment of canine osteosarcoma.

10

Using Methylene Blue Photodynamic Reaction to Obtain Cancer Vaccines

Murilo Del Grande, Maria Lucia Zaidan Dagli.
University of São Paulo, São Paulo, Brazil.

Introduction: Photodynamic Therapy (PDT) is a cancer treatment using laser to activate a photosensitizing agent delivered to the tumor. Known as Photodynamic Reaction (PR), it induces cell death mainly through apoptosis, especially Immunogenic Cell Death. Damage Associated Molecular Patterns released activate an adaptive immune response against remaining/metastatic cells. PR was used to obtain a cancer vaccine.

Experimental Design: Male BALB/c mice (7–8 week) were separated in two groups. Control = medium; PDT = vaccine (6 doses of 200 µl every 3 days). After 7 days, inoculation of B16F10 murine melanoma cells. Tumor growth was monitored for 15d. At necropsy tumor and spleen samples were processed for histology (H&E and "Anti-CD3" and "Anti-CD4"; Abcam®).

Methods: PDT Vaccine: 1x107 B16F10 cells/ml incubated with Methylene Blue (1µg/ml) in DMEM+10%FBS for 1 hour in humidified atmosphere of 5% CO_2 in air at 37°C. Irradiation with 660 nm red diode laser, 100 mW potency and 67.2 Joules energy dose, then incubated for 24 hours. Supernatant used as vaccine.

Results: Day 15 tumor volume: PDT = 2.640 ± 3.05; Control = 104.520 ± 61.51 (mean volume [mm^3] ± SD); significantly lower growth in vaccinated animals ($P<0,001$), also presenting spleen lymphoid hyperplasia. No differences on Lymphocyte T CD4+ and CD3+ spleen populations.

Conclusion: Methylene Blue Photodynamic Reaction produced an effective Vaccine against B16F10 murine melanoma.

Impact Statement: With further studies, PDT vaccines could be a valuable tool to treat veterinary and human cancer.

11

A Systematic Review of the Histopathologic Findings following Intraocular Recombinant Adeno-Associated Virus Vector Administration in Cynomolgus Macaques (*Macaca fascicularis*)

Annie Zimmerman[1,2], Ryan Boyd[2], Joshua Bartoe[2], Krishna Yekkala[2], Keith Nelson[2].

[1]*Michigan State University, Lansing, MI, USA.* [2]*MPI, Mattawan, MI, USA.*

Introduction/Objectives: Recombinant adeno-associated virus (rAAV) vectors are used for intraocular gene therapy of retinal degenerative diseases. Similarities in ocular anatomy, surgical approach, and vector dose make non-human primates (NHPs) an excellent model. Differentiation of procedure-induced findings from those of the vector or therapeutic gene is a key element of evaluating safety. A review of the histopathologic findings associated with intraocular rAAV administration in NHPs is presented here.

Methods/Experimental Design: A retrospective review of 100 animals from studies reported between 2011 and 2017 was performed.

Results: Intravitreal rAAV studies had inflammatory infiltrates in 32.5% of all dosed animals, including 11% of low dose and 61% of high dose animals, with none in controls. Findings were in the trabecular meshwork, anterior uvea, vitreous, and optic disc. Subretinal rAAV administration produced inflammatory infiltrates in 50% of all dosed animals, with no difference in incidence between low and high dose groups, and 21% of vehicle control animals. Vehicle group findings were limited to the subretinal space. Findings in dosed animals were seen in the subretinal space, vitreous, optic disc, and ciliary body, with high dose findings extending to the choroid and retina.

Conclusion: Intravitreal and subretinal rAAV administration is associated with dose-dependent increased intraocular inflammation and increased range of involved tissue compartments.

Impact Statement: Intraocular inflammation and secondary persistent reduction in visual acuity are reported in rAAV ocular gene therapy human clinical trials. Understanding of histopathologic lesion distribution following preclinical NHP rAAV delivery will guide future vector refinement and delivery techniques.

12

Repeated Administration of Cisplatin Increases EGFR/EGFR Activation and Renal Fibrosis in Kras4bG12D Lung Adenocarcinoma-Bearing Mice, but Kidney Injury Is Further Exacerbated with Erlotinib/Cisplatin Combination Treatment

Cierra Sharp[1], Mark Doll[1], Tess Dupre[2], Levi Beverly[1], Leah Siskind[1].

[1]*University of Louisville, Louisville, KY, USA.* [2]*University of Arizona, Tucson, AZ, USA.*

Cisplatin (CDDP) is a first choice therapy for many solid cancers, but 30% of patients develop acute kidney injury (AKI), which can progress to chronic kidney disease (CKD). Currently, there are no therapeutic interventions for CDDP-induced AKI or CKD. Clinically, only cancer patients receive CDDP, and it is administered in repeated, low doses to curtail CDDP nephrotoxicity. We optimized a repeated dosing model of CDDP (7 mg/kg 1x/wk for 4wks), which causes CKD in mice. To incorporate cancer into our model, we utilized a Kras4bG12D transgenic mouse that develops lung adenocarcinoma, and treated non cancer and cancer mice with repeated CDDP dosing. CDDP treated cancer mice had lower survival (50%), and worsened fibrosis indicated by Sirius red (SR) staining (25.4% SR +) and levels of myofibroblasts (α-SMA IHC; 4.6% +) compared to CDDP treated non cancer mice (11.6% SR +, 2.2% α-SMA +). Cancer mice treated with CDDP had increased EGFR and pEGFR Y1068 levels. We hypothesized that treating cancer mice with erlotinib (an EGFR inhibitor) in combination with CDDP would decrease EGFR activation and thereby decrease renal fibrosis. Administration of erlotinib (25 mg/kg once a day for 7 days) after a single dose of 7 mg/kg CDDP exacerbated renal damage and loss of function (NGAL: 1.30x10^6 pg/ml; BUN: 120 mg/dl) compared to the CDDP only group (NGAL: 4.99x105 pg/ml; BUN: 38.6 mg/dl). Data indicate erlotinib is not a viable renoprotective agent for CDDP-induced KI in our clinically relevant model.

13

Systematic Investigation of Sciatic Nerve Processing Parameters

Jessica S. Fortin[1], Elizabeth A. Chlipala[2], Daniel P. Shaw[1], Brad Bolon[3].
[1]*Veterinary Medical Diagnostic Laboratory, University of Missouri, Columbia, MO, USA.* [2]*Premier Laboratory (LLC), Boulder, CO, USA.* [3]*GEMpath Inc., Longmont, CO, USA.*

Introduction: Histopathological evaluation of the peripheral nervous system (PNS) is required for nonclinical safety studies done to register new chemical and pharmaceutical products. Current Society of Toxicologic Pathology (STP) "best practices" for PNS sampling, processing and analysis provide guidance regarding suitable methods for nerve examination, but some questions remain.

Objectives: The current study explores fixation and processing variables that may impact preservation of nerves.

Methods and Materials: Sciatic nerves were collected from adult rats and young pigs and immersed in neutral buffered 10% formalin (NBF, including 1.2% methanol as a stabilizing agent) or methanol-free 4% formaldehyde (MFF) at "0" (<15 min for rat and ~60 min for pig), 3, 6, 12, and 24 h at room temperature (RT). Nerve cross-sections were processed routinely into paraffin using incubation lengths of 10 or 40-60 min per station on an automated tissue processor, after which ~5-µm-thick H&E-stained sections were assessed for structural integrity and background findings.

Results: Fixation could be delayed for up to 3 h, after which myelin swelling occurred. The presence of methanol in the fixative (NBF) led to pallor and poor architectural definition in myelin sheaths. Large-caliber pig nerves required longer processing times per station (40–60 min) compared to small-caliber rat nerves (10 min).

Conclusions: Nerve processing is optimal when samples are fixed at RT in a methanol-free fixative within 3 h of death. Large-caliber nerves require longer processing cycles to ensure paraffin infiltration.

Impact Statement: These data provide additional information needed for optimal PNS processing.

14

The Impact of Different Assay Platforms on the Performance of Five Renal Injury Biomarker Assays for Rat Urine

Diane Hamlin, Albert Eric Schultze.
Eli Lilly and Company, Indianapolis, IN, USA.

Introduction: Commercial assays are available for many rat renal injury biomarkers, but the platforms may differ in reagents and/or detection mode. A study was conducted to investigate the effect of assay platforms on the performance of five rat renal injury biomarker assays.

Methods: Assays for urine Cystatin C, Kidney Injury Marker 1 (KIM1), Lipcalin-2 (LCN2), microAlbumin (µALb) and Osteopontin (OPN) on two platforms were compared.

Experimental Design: For each biomarker, urine samples from rats treated with vehicle or Gentamicin to induce tubular renal injury were tested on two assay platforms to investigate the impact on assay sensitivity, precision, and on the biomarker result fold-changes.

Results: Assay sensitivity was similar for both platforms for Cystatin C, KIM1, LCN2 and µALB, but one platform was more sensitive for OPN (8% vs 42% BQLs). Assay precision was acceptable and similar on both platforms for samples from naive rats and those with mid and high positive biomarker results. Imprecision was unacceptably high (30–88% CVs) for all urine biomarkers for a sample with low positive biomarker results when measured on one platform. The two platforms for all of the biomarkers provided similar fold-changes for the Gentamicin-treated rats vs controls, with correlations of 0.87–0.99.

Conclusions: In this study, the sensitivity and precision of the five renal injury biomarker assays were affected by the platform, but the biomarker result fold-changes for Gentamicin-treated vs vehicle control rats were not affected.

Impact Statement: Prior to use, the impact of the platform on assay performance should be evaluated.

15

Localization of Biomarkers in Murine Polycystic Kidney Disease by Tissue Mass Spectrometry Imaging

Dinesh Bangari, Cristina Silvescu, Laurie Smith, Lilu Guo, Mandy Cromwell, Sue Ryan, Petra Oliva, Alla Klos, Thomas O'Shea, Oxana Beskrovnaya, Beth Thurberg, Walter Korfmacher, Thomas Natoli.
Sanofi, Framingham, MA, USA.

Objective: To better understand the role of glycosphingolipid (GSL) accumulation in polycystic kidney disease (PKD) progression, we sought to characterize spatial distribution of GSLs in cystic kidneys of jck mice.

Methods: Fresh kidneys from C57Bl/6J (normal) and C57Bl/6J$^{nek8jck/jck}$ (jck) mice were embedded in gelatin, snap frozen, and cryosectioned at 10 µm. Tissue sections were mounted on Indium tin oxide-coated slides sprayed with MALDI matrix and subjected to mass spectrometry imaging (MSI); adjacent sections were stained with hematoxylin and eosin. Tissue MSI and MS/MS structural confirmation were performed with AB Sciex 4800 and Autoflex MALDI-TOF/TOF mass spectrometers.

Results: Tissue MSI revealed increased expression of GM3 gangliosides throughout jck kidney in comparison to normal mouse kidney. A hydroxylated form of GM3 was detected in blood vessels of the jck kidneys. Elevated levels of GM1 species were detected in jck kidneys in a patchy pattern that was distinguishable from that seen with GM3. Several sulfatide species could be detected in discrete patterns localizing to the cortex, medulla, and papilla; the C20 isoform was excluded from the papilla, while the C24 isoform was highly enriched in the papilla.

Conclusion: Accumulation of complex glycosphingolipids was assessed using tissue MSI in cystic kidneys compared to normal kidneys. Differences in either the carbohydrate composition of the GSL or the chain length of the lipid moiety affected their cellular localization.

Impact Statement: Tissue MSI provides a unique approach to elucidate the role and spatial localization of biomarkers related to murine PKD.

16

Elevation of Urinary MCP-1 in Patients with Acute Kidney Injury Receiving Lung Cancer Chemotherapy

Hiroyuki Watanabe, Mio Fukuda, Satohiro Masuda.
Department of Pharmacy, Kyushu University Hospital, Fukuoka, Japan.

Introduction: Acute kidney injury (AKI) is a common and serious adverse reaction of platinum-based chemotherapy. Serum creatinine level and estimated glomerular filtration rate (eGFR) are considered routine laboratory parameters to evaluate kidney function. However, specific and sensitive biomarkers are additionally required to assess drug-induced nephrotoxicity. This study aimed to determine suitable urinary biomarkers among several recently discovered candidate molecules, including monocyte chemotactic protein-1 (MCP-1) and neutrophil gelatinase-associated lipocalin (NGAL), for the rapid detection of platinum-induced AKI in lung cancer patients.

Experimental Design: Urine samples were obtained from 18 (8 AKI-positive [+] and 10 AKI-negative[-]) patients with lung cancer 1 d before treatment with cisplatin or carboplatin, and subsequently on days 3, 7, and 14 after treatment. Urinary MCP-1 and NGAL levels were determined using specific enzyme-linked immunosorbent assay kits for each marker.

Methods: Urinary levels of these molecules were compared and analyzed using area under the curve and receiver operating characteristic curve (AUC-ROC) analyses. Differences were compared using Mann-Whitney's U test, and p values of <0.05 were considered statistically significant.

Results: Urinary MCP-1 in the AKI (+) samples were significantly higher than those in the control samples ($p<0.05$), while urinary NGAL levels were not significantly increased in AKI samples. Additionally, the AUC-ROC of MCP-1 and NGAL were 0.68 ($p < 0.05$) and 0.62 ($p > 0.05$), respectively.

Conclusions: Urinary MCP-1 is a potentially effective biomarker for platinum-induced AKI in lung cancer patients.

Impact Statement: Urinary MCP-1 may support classical parameters in the rapid detection of drug-induced nephrotoxicity.

17

A Mouse Model of Immune-Complex Mediated Vascular Disease

Lykke Boysen[1,2], Lone H. Landsy[3], Birgitte M. Viuff[1], Jens Lykkesfeldt[2], Brian Lauritzen[1].

[1]*Toxicology, Safety Pharmacology and Toxicopathology, Non-clinical Development, Novo Nordisk A/S, Måløv, Denmark.* [2]*Experimental Pharmacology and Toxicology, Faculty of Health and Medical Sciences, University of Copenhagen, Frederiksberg, Denmark.* [3]*Immunogenicity Assessment, Non-clinical Development, Novo Nordisk A/S, Måløv, Denmark.*

Introduction: In development of new biopharmaceuticals, dosing human proteins to animals, potentially leads to formation of anti-drug-antibodies (ADAs), which together with the drug may form immune-complexes (ICs). If large amounts of ICs are formed, intrinsic clearance mechanisms may be overwhelmed, eventually leading to vascular IC-deposition and inflammation. Thus, we aimed to develop a mouse model of IC-mediated vascular disease and to identify biomarkers of IC-deposition.

Experimental Design: Female C57BL/6J mice were dosed 10 mg/kg Adalimumab s.c. twice weekly for 6 weeks. Hereafter, dose levels were changed to 100, 10 or 1 mg/kg or 10 mg/kg four times weekly for 7 weeks. A control group received vehicle twice weekly for 13 weeks (n=12/group). Blood was sampled after 6 and 13 weeks and kidneys harvested at week 13.

Methods: Exposure was measured by Luminescent Oxygen Channelling Immunoassay. ADA-Adalimumab complexes and complement bound circulating ICs (CICs) were measured by ELISA. IC-deposition and histopathological changes were evaluated by IHC and HE-PAS stain.

Results: Administration of Adalimumab to mice induced ADA and CIC-formation, which led to vascular deposition of ICs containing hIgG, mIgG, mIgM, and C3, as well as glomerulonephritis. Preliminary data indicate consistency between increases in ADA-CIC and IC-deposition in the vasculature.

Conclusion: An animal model of IC-mediated vascular disease has been established, and ADA-CIC identified as possible biomarkers of IC-deposition.

Impact Statement: Establishment of an animal model of IC-mediated vascular disease and identification of biomarkers for IC-deposition may improve interpretation and translatability of IC-related findings in animal studies.

18

Validation of Flow Cytometry-Based Quantitation of Reticulated Platelets in Cynomolgus Monkeys and Wistar Rats

Madhu Sirivelu[1], Deborah Carraher[1], Kim Lewis[1], James Warneke[1], Rodrigo Laureano[1], William Reagan[2], Laurence Whiteley[1].

[1]*Pfizer, Inc., Andover, MA, USA.* [2]*Pfizer, Inc., Groton, CT, USA.*

Introduction: Decrease in platelets is one of the most common hematologic effects of novel drug entities, especially biotherapeutics. Measurement of reticulated platelets (immature platelets with higher RNA content) helps assess the effects of therapeutics on thrombopoiesis. The objective of this study is to describe a fit-for-purpose validation of a flow cytometry-based assay to measure reticulated platelets in common preclinical species, monkeys, and rats.

Experimental Design: Male cynomolgus monkeys were administered Compound X (75 mg/kg/day for 9 days; recovery period of 15 days) and male Wistar Han (Crl: WI[HAN]) rats were administered cyclophosphamide (25 mg/kg/day for 3 days; recovery period of 19 days) and E.coli lipopolysaccharides (LPS; 2 mg/kg once; recovery period of 21 days). These compounds are known to affect platelet production.

Methods: Reticulated platelets were assessed by flow cytometry using CD41, CD61 markers and thiazole orange. Assay performance was evaluated based on intra-assay precision, stability, and specificity.

Results: Performance results of flow cytometry-based reticulated platelet assay was within acceptance criteria with intra-assay precision of 5.8%–6.1% and 3.6%–3.8%, stability for 3 and 6 hours, in monkeys and rats respectively. In both species, the specificity was determined by treatment with RNAse. Changes in reticulated platelets corresponded to the effect of test articles on platelet production.

Conclusion: Flow cytometry-based reticulated platelet assay is a sensitive and specific assay for assessing thrombopoiesis with acceptable performance characteristics.

Impact Statement: Reticulated platelet assay is a sensitive tool to monitor changes in platelet production in preclinical species.

19

Evaluation of the Flavonoid Antioxidants, *alpha*-Glycosyl Isoquercitrin and Isoquercetrin, for Genotoxic Potential

Cheryl Hobbs[1], Mihoko Koyanagi[2], Carol Swartz[1], Jeffrey Davis[1], Sawako Kasamoto[3], Robert Maronpot[4], Leslie Recio[1], Shim-mo Hayashi[2].
[1]*Integrated Laboratory Systems, Inc., Research Triangle Park, NC, USA.* [2]*San-Ei Gen F.F.I., Inc., Osaka, Japan.* [3]*Public Interest Incorporated Foundation Biosafety Research Center, Shizuoka, Japan.* [4]*Maronpot Consulting LLC, Raleigh, NC, USA.*

Introduction: Quercetin and its glycosides are thought to possess potential benefits to human health. Several flavonols are available to consumers as dietary supplements, promoted as anti-oxidants; however, incorporation of natural quercetin glycosides into food and beverage products has been limited by poor miscibility in water. Enzymatic conjugation of multiple glucose moieties to isoquercitrin to produce *alpha*-glycosyl isoquercitrin (AGIQ) has been shown to enhance solubility and bioavailability. AGIQ is used in Japan as a food additive and has been granted generally recognized as safe (GRAS) status. However, although substantial genotoxicity data exist for quercetin, there is very little available data for AGIQ and isoquercitrin.

Experimental Design: To support expanded global marketing of food products containing AGIQ, comprehensive GLP-compliant testing of the genotoxic potential of AGIQ and isoquercitrin was conducted in accordance with current regulatory test guidelines.

Results: Both chemicals tested positive in reverse mutation assays in several bacterial strains with and without metabolic activation, and 4-hour, but not 24-hour, exposure to isoquercitrin resulted in chromosomal aberrations in CHO-WBL cells in the presence and absence of metabolic activation. All other *in vitro* mammalian micronucleus and chromosomal aberration assays, micronucleus and comet assays in male and female B6C3F1 mice and Sprague-Dawley rats, and mutation assays evaluating multiple potential target tissues in transgenic Muta™ Mice were negative for both chemicals.

Conclusion/Impact Statement: These results demonstrate a lack of *in vivo* genotoxicity of AGIQ and supplement existing toxicity data to further support its safe use in food and beverage products.

20

Histomorphologic Patterns of Toxicity Associated with Seven Renal Toxicants in NHP and Their Urinary Biomarker Correlates

Sean Troth[1], Katerina Vlasakova[1], Yi-Zhong Gu[1], Jarig Darbes[2], Flavia Pasello dos Santos[2], Takayuki Tsuchiya[1], Robert Peiffer[1], Frank Sistare[1], Warren Glaab[1].
[1]*Merck, West Point, PA, USA.* [2]*MSD, Mirabel, France.*

Introduction: To date a majority of renal biomarker research has been conducted in rat with a relative paucity of information regarding nonhuman primate (NHP) as a model of acute kidney injury. NHP are an important nonclinical model for assessing drug-induced injuries based on their close evolutionary relationship with humans. A series of studies were conducted in NHP assessing histomorphologic patterns of renal injury and corresponding urine biomarker changes using 7 drugs associated with nephrotoxicity (cefpirome, gentamicin, everninomicin, cisplatin, naproxen, tenofovir, and cyclosporine).

Experimental Design/Methods: Six exploratory NHP studies were conducted in *Macaca mulata* (rhesus) or *Macaca fascicularis* (cynomolgus) treated daily for 7 to 14 days intravenously (everninomicin, gentamicin, cefpirome, cisplatin and tenofovir), subcutaneously (cyclosporine) or by oral gavage (naproxen). Urine (for urinary creatinine, albumin, total protein, NAG, KIM-1, OPN, NGAL, RBP4, Cystatin C, Clusterin) and serum (BUN and SCr) samples were collected pretest and at intervals throughout the study. Histomorphologic evaluation of kidney was conducted at the end of the treatment period and (gentamicin, everninomicin and cisplatin) following a treatment free period.

Results: Histomorphologic features observed following treatment were generally consistent with analogous drug-induced changes in humans described in the literature. The biomarkers were useful for detecting drug-induced renal tubular injury in NHP, with Kim-1 and clusterin showing the highest overall performance.

Impact Statement: These findings demonstrate the utility of urinary kidney translational safety biomarkers in nonhuman primates and provide additional supporting evidence for translating these biomarkers for use in clinical settings to further ensure patient safety.

21

Measurement of Urea Nitrogen in Broncho-Alveolar Lavage Fluids (BALF) in Nonhuman Primates (NHP)

Virginie Allegret, Luc Huard, Jeffrey McCartney, Rina Massarelli, Florence Poitout.
Charles River Laboratories, Senneville, QC, Canada.

Introduction/Objectives: In preclinical studies, BALFs are frequently collected for toxicokinetic studies of inhaled drugs, and for determination of cytokines or chemistry analytes. The measurement of urea nitrogen (UN) in BALF is used to determine the amount of dilution of the fluid adjacent to epithelial lining cells (ELF) following lavage procedure. Because urea is a small molecule easily diffusible through epithelial cells, it is considered to be of equal concentration in serum and ELF. However, UN concentration in BALF is generally below the limits of quantification when evaluated with blood urea nitrogen (BUN) method on a chemistry analyzer, and its measurement necessitated to adapt an automated method for BUN.

Methods and Materials: UN was measured using the Cobas 6000 c501 (Roche Diagnostics) analyzer; the enzymatic method, a kinetic test with urease and glutamate dehydrogenase, was adapted to run BALF samples.

Results: This validation demonstrated that the method was linear (R2 = 0.99), sensitive (LOD = 0.110 mg/mL and LLOQ=0.170 mg/dL), and precise (intra-assay %CV: 3.8–19.0 and inter-assay %CV: 4.0–14.1), and UN was stable in BALF for 1 day at room temperature and 4°C, for 7 days at -20°C and following two freeze/thaw cycles. Individual BALF UN values were 0.56–0.89 mg/dl.

Conclusion: Measurement of UN in BALF using an adapted automated assay, originally designed to determine BUN, is a robust method allowing the calculation of the ratio BALF UN/serum UN that serves as an indicator of BALF dilution in cynomolgus monkeys.

22

INHAND: International Harmonization of Nomenclature and Diagnostic Criteria for Lesions—An Update—2018

Charlotte Keenan[1], John Vahle[2], Dawn Goodman[3], Emily Meseck[4], Ronald Herbert[5], Alys Bradley[6], Matt Jacobsen[7], Rupert Kellner[8], Susanne Rittinghausen[8], Christine Ruehl-Fehlert[9], Thomas Nolte[10], Shim-mo Hayashi[11], Takanori Harada[12], Katsuhiko Yoshizawa[13]. [1]*CM Keenan ToxPath Consulting, Doylestown, PA, USA.* [2]*Eli Lilly & Company, Indianapolis, IN, USA.* [3]*Independent Consultant, Potomac, MD, USA.* [4]*Novartis Institute for Biomedical Research, East Hanover, NJ, USA.* [5]*NIEHS, Research Triangle Park, NC, USA.* [6]*Charles River Laboratories, Tranent, East Lothian, United Kingdom.* [7]*AstraZeneca, Alderley Park Macclesfield, United Kingdom.* [8]*Fraunhofer ITEM, Hannover, Germany.* [9]*Bayer Schering Pharma AG, Wuppertal, Germany.* [10]*Boehringer Ingelheim Pharma GmbH & Co. KG, Biberach an der Riss, Germany.* [11]*San-Ei Gen F.F.I, Inc., Ikuno Osaka, Japan.* [12]*The Institute of Environmental Toxicology, Joso-shi, Ibaraki, Japan.* [13]*Mukogawa Women's University, Nishinomiya, Hyogo, Japan.*

The INHAND Proposal (International Harmonization of Nomenclature and Diagnostic Criteria for Lesions in Rats and Mice) has been operational since 2005. A Global Editorial Steering Committee (GESC) helps coordinate overall objectives of the project. Development of harmonized terminology for each rodent organ system or non-rodent species is the responsibility of the Organ Working Groups (OWG) or Non-rodent Working Groups (NRWG) respectively, drawing upon experts from North America, Europe and Japan.

Great progress has been made with 14 rodent organ systems published to date—Respiratory, Hepatobiliary, Urinary, Central/Peripheral Nervous Systems, Male Reproductive and Mammary, Zymbals, Clitoral and Preputial Glands in *Toxicologic Pathology* and the Integument and Soft Tissue, Female Reproductive System, Digestive System, Cardiovascular System, Skeletal System, Special Senses and Endocrine System in the *Journal of Toxicologic Pathology* as supplements and on a website—**www.goReni.org**. Recommendations of the Apoptosis/Necrosis Working Group have been published. INHAND guides offer terminology, diagnostic criteria, differential diagnoses and guidelines for recording lesions in toxicity and carcinogenicity studies. The guides provide representative photo-micrographs of morphologic changes, information regarding pathogenesis, and key references.

INHAND GESC representatives attend meetings with representatives of FDA Center for Drug Evaluation and Research (CDER), Clinical Data Interchange Standards Consortium (CDISC), and National Cancer Institute (NCI) Enterprise Vocabulary Services (EVS) to assist with incorporating INHAND terminology as preferred terminology for SEND (Standard for Exchange of Nonclinical Data) submissions to the FDA. Interest in INHAND nomenclature, based on input from industry and government scientists, is encouraging wide acceptance of this nomenclature.

23

Interpretation of Organ Weight Changes in a Rat Preweaning Juvenile Toxicity Study with Negative Growth Effects

Cindy Fishman[1], Lorrie Posobiec[1], Susan Laffan[1], Mark Price[2], Dinesh Stanislaus[1], Jeffrey Charlap[3], Michelle Elliott[3].
[1]*GlaxoSmithKline, King of Prussia, PA, USA.* [2]*GlaxoSmithKline, Ware, United Kingdom.* [3]*Charles River, Horsham, PA, USA.*

Introduction: Juvenile toxicity studies evaluate developing organ systems.

Methods: Rats were dosed orally with an immunomodulatory agent from postnatal day (PND) 4-22 with an 11-week off-dose period to PND 106, supporting children from preterm birth to 2 years.

Results: At PND22, the highest dose caused decreased body weight gain (0.79X control), considered non-specific toxicity with presumed decreased suckling. Femurs were shorter (to 0.95X), supporting general hindrance of growth.

At PND 22, absolute weights of most organs decreased in proportion to body weight. However, absolute brain weights were decreased (0.88X) with increased brain weights relative to body weights (1.06X), representing partial sparing of the brain compared to the body.

At PND 106, body weights and most organ weights were like control. Femurs remained shorter (0.95X). Absolute brain weights remained decreased (0.87X), now with similar decreases in brain weight relative to body weight.

At PND 22, absolute heart weights were unaffected, with increased heart weights relative to body weight (to 1.29X). At PND 106, absolute and relative heart weights were like control. PND 22 findings were considered related to normal rapid growth of the heart compared to the body in the early postnatal period in rats, with the heart entirely spared from negative growth effects.

Conclusion: These data align with human and animal literature demonstrating undernutrition during critical periods of growth results in irreversible effects on stature and intelligence.

Impact Statement: These data reinforce the importance of understanding differential effects of growth hindrance when interpreting organ weights in juvenile animals.

24

Characterization of Endometrial Stromal Polyp Subtypes in the Rat

Erin Quist[1], Daven Jackson-Humbles[2], Karen Cimon[1], Lauren Shelby[3], Mark Cesta[2], Norris Flagler[2], Gabrielle Willson[1], Ron Herbert[2], Darlene Dixon[4].
[1]*Experimental Pathology Laboratories, Inc., Durham, NC, USA.* [2]*Cellular and Molecular Pathology Branch, National Toxicology Program, National Institute of Environmental Health Sciences, Research Triangle Park, NC, USA.* [3]*College of Veterinary Medicine, Kansas State University, Manhattan, KS, USA.* [4]*NTP Laboratory Branch, National Toxicology Program, National Institute of Environmental Health Sciences, Research Triangle Park, NC, USA.*

Introduction: Criterion established by the International Harmonization of Nomenclature and Diagnostic Criteria (INHAND) separates endometrial polyps into two subtypes: "polyp, glandular" and "polyp, endometrial stromal." *"Polyp, glandular"* consists predominantly of an often hyperplastic, glandular component of cuboidal to columnar epithelium continuous with, and similar in appearance to, the endometrial mucosal epithelium; whereas "*polyp, endometrial stromal*" is mainly composed of stromal spindle or stellate cells with no or very few glandular elements.

Objectives: 1) Determine more definitive criteria for distinguishing polyp subtypes, 2) determine if the morphology of each subtype remains consistent throughout all levels of the polyp, and 3) determine if polyp subtype may indicate biological behavior.

Experimental Design: Rat polyp samples obtained from NTP Archives were categorized as follows: polyp, glandular (20); polyp, stromal (20); and polyp, cystic stromal (15), a previously uncharacterized subtype. 5 µm step-sections were obtained every 100 µm to a total depth of 500 µm. H&E sections from each level were used to evaluate consistency of polyp morphology and for morphometric analysis.

Results: Preliminary morphometric analysis indicated that the glandular subtype contained larger numbers of glandular units (mean = 233.7) than the stromal (mean = 79.85) or cystic stromal subtypes (mean = 73.67). In addition, the mean total area (mm^2) varied based on polyp subtype where stromal (44.56) > cystic stromal (32.86) > glandular (22.15).

Future Directions: IHC staining will be used to assess proliferation indices and determine if differential staining exists among polyp subtypes, providing additional information on subtype origin and biological behavior.

25

Retrospective Analysis of Fungal Rhinitis in Sprague-Dawley Rats: A Decade of Carcinogenicity Studies

Jennifer Lamoureux[1], Karen Carlton[2], Charissa Dean[1], Keith Nelson[1].
[1]MPI Research, Mattawan, MI, USA. [2]University of Guelph, Guelph, ON, Canada.

Introduction: Fungal rhinitis is observed in chronic toxicology studies in rodents and may contribute to premature deaths, thereby confounding interpretation of toxicologic findings. Fungal rhinitis has been linked to cage microenvironment, inhalation of dust from bedding or food, or concurrent viral or bacterial infections, as well as immunosuppression, and/or stress from handling.

Experimental Design: We retrospectively evaluated data from thirty-two Sprague-Dawley rat 2-year carcinogenicity studies conducted over a decade, including 25,781 animals, for findings of fungus and inflammation within the nasal cavity. In each, four H&E-stained sections of the nose were examined.

Results: Fungus uniformly had septate, parallel walls, and dichotomous branching, with occasional fruiting bodies, consistent with *Aspergillus sp*. Inflammation consisted of mixed leukocytes, predominately neutrophils. Respiratory epithelial hyperplasia, squamous metaplasia, and epithelial ulceration were occasionally observed. The overall incidence was similar between treated and untreated animals, with males more frequently affected than females (untreated males 2.7% vs. treated males = 2.97% and untreated females = 0.028% vs. treated females = 0.034%). Incidence was generally low (< 1%), although there was variance over time and up to 9.6% incidence was seen in one study. There was no correlation between fungus/inflammation with the incidence of neoplasia within the nasal cavity. Occasionally, fungal rhinitis was the proximate cause of morbidity/early euthanasia.

Conclusion: Fungal rhinitis occurs with low incidence as a background finding, most frequently in males. Clinical or subclinical manifestations can lead to morbidity/early euthanasia but there is no increased incidence of nasal cavity neoplasia.

26

Pathological Changes—Including Cardiovascular Changes—In Cynomolgus Monkeys Induced by Anti-CD47 Monoclonal Antibody

Ke Chen[1,2,3], Shuang Qiu[1,2], Tao Chen[1,2], Peter Mann[4], Xiaobo Cen[1,2,3].
[1]Westchina-Frontier Pharma Tech Co., Ltd., Chengdu, China. [2]National Chengdu Center for Safety Evaluation of Drugs, Chengdu, China. [3]West China School of Medicine, West China Hospital, Sichuan University, Chengdu, China. [4]Experimental Pathology Laboratories, Inc., Seattle, WA, USA.

Introduction: CD47 is an inhibitory membrane protein regulates phagocytosis mediated by cells of the innate immune system. Cancers use CD47 as a "don't-eat-me" signal to escape from being eaten and eliminated by the macrophages.

Experimental Design: Cynomolgus monkeys were administrated via intravenous injection twice a week for 4 consecutive weeks.

Methods: Hematology, clinical chemistry, lymphocyte subsets data were collected during the in life phase. Animals were euthanasia, organ weights data was collected and bone marrow smears was performed. 48 organs/tissues were collected from each monkeys for histopathologic examination.

Results: Increased size and organ weight of the spleen and decreased size and weight of thymus were noted. Microscopically, decreased lymphocytes in the thymus and spleen, centrilobular hepatocellular hypertrophy, Kuffer cell pigmentation and extramedullary hematopoiesis(EMH) in the liver, hyperplasia in the bone marrow were observed. Above changes were consistent with the in life results. Moreover, artery hypertrophy/hyperplasia, thrombus/recanalization and secondary infarct were noted in the lung/synovium/salivary gland/heart, red pulp congestion in the spleen was also noted.

Conclusion: The microscopic changes were consistent with increased RET, RET%, TBIL, CD3+CD4+/CD3+CD8+ T cells ratio, and decreased RBC, HGB, HCT, PLT, CD3+CD8+ T cell count noted in-life. Anti-CD47 antibody induced hemolysis which caused pigmentation, EMH and compensatory bone marrow hyperplasia. It also affected the T cells, especially CD8+ T cells, caused decreased lymphocytes in the thymus. In particular, it induced several cardiovascular changes, including artery hypertrophy/hyperplasia, thrombus/recanalization and congestion

Impact Statement: This is the first report on the cardiovascular changes caused by anti-CD47 antibody. It reminds the investigator of the potential cardiovascular risk when the clinical trials conducted on humans.

27

Cathepsin K Inhibitor Associated with Minimal Change-Like Renal Changes in Rhesus Monkeys

Laura Gumprecht.
Merck & Co., Inc., West Point, PA, USA.

Cathepsin K is a cysteine protease found primarily in osteoclast lysosomes and is responsible for degradation of demineralized bone matrix in the bone remodeling process. Cathepsin K inhibitors have been developed for the treatment of osteoporosis and other bone-related indications. A cathepsin K inhibitor was tested in a 3-month toxicity study in rhesus monkeys. Male and female monkeys were administered vehicle or compound orally at 5, 15, or 45 mg/kg/day for 30 days. Within 4–5 weeks high dose monkeys had decreased activity, distended abdomens, swelling of the face and urogenital area, and were euthanized. The remainder of the monkeys in the dose group was euthanized in Drug Week 6. Clinical pathology changes included decreased serum protein, albumin and A/G ratio; increased BUN and creatinine; and proteinuria. Gross findings included clear fluid in the thoracic and abdominal cavities, pale and soft kidneys, watery content in the large intestine, and edema in multiple tissues. By light microscopic evaluation high dose monkeys had glomerulopathy, and tubular changes included dilation, degeneration, and proteinaceous accumulation. Ultrastructurally, glomeruli had podocyte foot process effacement and microvillus formation. It was subsequently determined that this basic, lipophilic compound accumulated in lysosomes and its effects in the kidney were likely related to off-target toxicity. To summarize, administration of this cathepsin K inhibitor, which was unexpectedly lysosomotropic, induced glomerulopathy and renal toxicity consistent with minimal change disease.

28

Incidence of Atypical Wistar Rat Advia® Cytograms and the Effects on Select Hematology Parameters at Covance-Madison

Mandy Meindel, Holly Jordan, Laura Wieczorkiewicz.
Covance, Madison, WI, USA.

Introduction: Erythrocyte agglutination in Wistar rats is associated with glutaraldehyde in the Siemens Advia® 2120i Hematology System red blood cell reagent. This causes atypical cytograms and effects on mean corpuscular volume (MCV), red cell distribution width (RDW), and red blood cell concentration (RBC) from the red blood cell channel, but not the reticulocyte channel. We evaluated the incidence of this phenomenon in our facility.

Methods: Advia® cytograms from 76 female and 74 male control Wistar rats were evaluated and effects on MCV, RDW, and RBC in both channels were compared.

Results: 26.7% of control rats had atypical cytograms (17.1% of females; 36.5% of males). In these rats, RDW and MCV were generally higher and RBC was generally lower in the red blood cell channel v. reticulocyte channel. RDW was 27.8% higher in the red blood cell channel compared with 3.8% for unaffected rats. MCV was 3.3% higher in the red blood cell channel compared with 1.8% for unaffected rats. RBC was 4.4% lower in the red blood cell channel compared with 1.3% for unaffected rats.

Conclusion: Agglutination was detected in 36.5% of male and 17.1% of female control Wistar rats. Effects were most pronounced on RDW (higher) with lesser effects on MCV (higher) and RBC (lower).

Impact Statement: Because glutaraldehyde-induced agglutination affects Advia® results for many Wistar rats when using the red blood cell channel, hematology from this strain should be reported from the Advia® reticulocyte channel.

29

Necrohemorrhagic Pneumonia Caused by Extraintestinal *Escherichia coli* in Multiple Research Dogs

Michelle Magagna[1], April George[2], Caitlyn Carter[2], Charissa Dean[2], Keith Nelson[2].
[1]*Michigan State University Veterinary Diagnostic Laboratory, Lansing, MI, USA.*
[2]*MPI Research, Mattawan, MI, USA.*

Introduction: Pneumonia is an uncommon but serious cause of morbidity in beagle research dogs. It is often associated with pulmonary misdosing or potential test-article effects, rather than infectious etiologies. Extraintestinal pathogenic *Escherichia coli* is a rarely reported cause of acute, fatal necrohemorrhagic pneumonia, particularly strains expressing cytotoxic necrotizing factor (CNF) 1 and 2 virulence factors.

Experimental design: Cases of acute necrohemorrhagic pneumonia in beagle dogs at MPI Research between 2011–2017 were reviewed.

Methods: Clinical presentation, macroscopic and microscopic findings, and laboratory testing results in 13 dogs (8 male, 5 female) with suspected pneumonia were reviewed and compared.

Results: Almost all dogs died or were euthanized *in extremis* after a short course of clinical symptoms or following receipt from suppliers. Clinical symptoms were typically fulminant, consisting of lethargy, dyspnea, and hemorrhage. In all dogs, affected lung lobes were variably discolored dark red. Few dogs had pleural effusion and multisystemic hemorrhage. Pulmonary histologic lesions included alveolar necrosis, hemorrhage, edema, fibrin deposition, acute inflammation, and intralesional colonies of bacterial bacilli. Nine dogs were cultured and isolated *E. coli*; for 7 of these dogs, virulence factor PCR was performed and identified CNF-1 (no other factors identified).

Conclusion: Extraintestinal is an emerging, important cause of acute necrohemorrhagic pneumonia in purpose-bred beagle research dogs, and may often be associated with a recent history of transport.

Impact Statement: This case series provides evidence that should be considered as a potential cause of acute fatal respiratory disease in beagle research dogs.

30

Tube Type and Centrifugation Conditions Contribute to Hemolyzed Serum Samples in Rats

Mike Logan, Tammy Palenski, Samantha Wildeboer, Sue Riendl, Irina Skarzhin, Dimple Patel, Joslyn Lewis, Kelly Robinson, Kirstin Barnhart.
AbbVie, North Chicago, IL, USA.

Introduction: An investigation was performed to determine how tube type and centrifugation conditions contribute to hemolysis in clinical chemistry samples from rats.

Experimental Design: Blood from 10 (5 male/5 female) Sprague-Dawley (SD) rats was collected and aliquoted into K^2EDTA and four different serum collection tubes. Blood from the serum collection tubes was processed to serum using one of two different centrifugation protocols to assess how tube volume, inclusion of serum separator gel, and centrifugation affected hemolysis.

Methods: K^2EDTA blood was used to assess routine hematology parameters, osmotic red blood cell (RBC) fragility, and mechanical RBC fragility. Serum aliquots from each tube were evaluated for clinical chemistry parameters and hemolytic index. Clinical chemistry and hemolytic index data were compared to the laboratory's current centrifugation conditions and tube size/type (designated control).

Results: Compared to females, male RBCs had more hemolysis after exposure to the mechanical fragility model. Compared to control, serum from small volume tubes and serum from tubes centrifuged at lower speed and shorter duration had lower mean hemolytic index values, decreased lactate dehydrogenase activities, and aspartate aminotransferase activities. The absence of a serum separator gel had no effect on hemolytic index or enzyme activity.

Conclusions: Serum tube selection and centrifugation conditions can contribute to hemolysis in SD rat serum samples. Smaller tubes and slower centrifugation speeds resulted in less hemolysis.

Impact Statement: Tube selection and centrifugation conditions provide opportunities to control hemolysis, an important contributor to pre-analytical variability, in SD rat serum samples.

31

Spontaneous True Hermaphroditism in a Sprague-Dawley Rat

Norifumi Takimoto[1], Noriaki Ishigami[1], Kenji Nakamura[2], Atsuko Murai[2], Kengo Namiki[2], Daisuke Hibi[1], Koji Shimouchi[1].

[1]*Ono Pharmaceutical Co., Ltd., Osaka, Japan.* [2]*Ono Pharmaceutical Co., Ltd., Fukui, Japan.*

Introduction: True hermaphroditism is defined by the presence of an ovotestis (unilateral or bilateral) or an ovary on one side and a testis on the contralateral side. Spontaneous true hermaphroditism is rare in rats. We encountered a case of true hermaphroditism in a Crl: CD(SD) rat and histopathologically examined this animal.

Materials and Methods: We purchased this animal presumed as male at 4 weeks old. Since there was a vaginal-orifice-like structure in the vulva, we collected a vaginal smear at 26 weeks old and autopsied this animal at 27 weeks old.

Results: There was no apparent penis, and the scrotum had not been developed. During the rearing period, urine was excreted from a vaginal-orifice-like structure, and a clitoral-like structure was observed to be gradually enlarged and protruded. The vaginal smear showed the diestrous stage. At autopsy, gonads were present where ovaries are located in normal female rats. Histologically, we diagnosed both gonads as ovotestes because of a mixture of atrophic tubules and granulosa cells. An oocyte was present in the left ovotestis. On each side, an epididymis, a deferent duct, a uterine horn, accessory reproductive glands (seminal vesicle, prostate and bulbourethral glands), and a preputial/clitoral gland were found. Beside the right ovotestis, an oviduct was present. Osteoid tissue was formed in the clitoral-like structure. There was no apparent spermatogenesis.

Conclusion: In this animal, there were ovotestes characterized by atrophic tubules and granulosa cells. Therefore, we diagnosed it as bilateral true hermaphroditism.

32

Age-Related Changes in Hematopoietic Activity in the Bone Marrow, Spleen, and Liver in Neonatal, Juvenile, and Young/Adult Göttingen Minipigs

Pierluigi Fant[1], Marjolein van Heerden[2].

[1]*Charles River, Lyon, France.* [2]*Janssen Research & Development, Beerse, Belgium.*

Introduction: With the increased use of juvenile minipigs, there is a need to document age-related microscopic changes.

Experimental Design: 57 neonatal minipigs received water or cyclodextrin orally from postnatal day 1 or were untreated. Scheduled euthanasias occurred on day 14, 35, or 63.

Methods: Spleen and liver weights and histopathology of spleen, liver, sternum and femur were evaluated. Findings were compared with control young/adult pigs (> 5 months old) from previous studies.

Results: Increases in spleen and liver absolute and relative weights in neonatal/juvenile pigs were generally more pronounced between day 35 and 63. Microscopically, hepatic extramedullary hematopoiesis (EMH) was minimal/slight on day 14, minimal/absent on day 35, and absent by day 63. Minimal/slight hemosiderin deposits in the liver were noted at each time-point. In the spleen, EMH was generally marked on day 14, minimal/absent on day 35, and absent by day 63. Scattered "tingible body" macrophages were seen in the spleen on day 14. Bone marrow cellularity in sternum and femur was high and scattered "tingible body" macrophages were observed on day 14 and 35. In young/adult pigs, EMH in the spleen and liver was generally absent, and fat tissue in bone marrow was variably increased.

Conclusion: Notable age-related changes occurring in the first 2 months of age were observed in spleen and liver weights and in the microscopic appearance of the spleen, liver and bone marrow.

Impact Statement: Background data on hematopoietic organs support evaluation of juvenile minipigs in toxicity studies.

33

Liver Hypertrophy and Toxicity to Microcystin-LR: Gender Differences in CD-1 Mice following Oral Administration

Shambhunath Choudhary[1], Mark Morse[1], Christopher Weghorst[2], Thomas Knobloch[2], Igor Mrdjen[2], Randy Ruch[3], Jiyoung Lee[2].
[1]*Charles River Laboratories, Spencerville, OH, USA.* [2]*Ohio State University, Columbus, OH, USA.* [3]*University of Toledo, Toledo, OH, USA.*

Introduction/Objectives: Microcystin-LR (MCLR) is a potent hepatotoxin produced during cyanobacterial blooms in freshwater sources. The toxicity of MCLR has been previously characterized in mice, but most of the earlier studies were conducted in a single-sex, by the intraperitoneal route of administration and, in some cases, the purity of MCLR was questionable.

Experimental design: In order to better characterize the toxicity of MCLR in mice using a human-relevant route of administration, groups of 10 male and female CD-1 mice were administered MCLR via oral gavage at dose levels of 0, 3000, and 5000 µg/kg/day for up to 7 days.

Results: Mortality reached 30% (3/10) in females as compared to a single death in males. Clinical chemistry parameters were also more prominent in females and included significant elevations in AST (up to 4.1X in males and 13.0X in females) and ALT (up to 10.7X in males and 24.8X in females) compared to the respective controls. Histopathological findings in early deaths included marked hemorrhage/necrosis and in mice that survived to scheduled euthanasia included dose-dependent centrilobular hepatic necrosis/degeneration and hepatocellular hypertrophy; the incidence of hepatocellular hypertrophy was higher in male mice.

Conclusion: Higher constitutive GST activity/GSH levels in male CD-1 mice, which detoxify MCLR, likely contributed to the higher incidence of hepatic hypertrophy and reduced susceptibility to MCLR toxicity.

Impact Statement: To the authors' knowledge, this is the first published report of a sex difference in hepatic hypertrophy and toxicity in mice following oral MCLR exposure.

34

Nucleoside/tide Inhibitors—Mitochondrial Toxicity or Other Mechanisms?

Sherry Morgan, Michael Liguori, Rich Peterson, Mike Logan, Meg Ramos, George Foley.
AbbVie, North Chicago, IL, USA.

Introduction/Objective: Nucleoside/tide inhibitors have been developed as therapies for a variety of life-threatening viral diseases. While often offering the advantage of a high barrier to viral resistance, in several instances they have been associated with significant toxicity, resulting in development discontinuation or withdrawal from the market. The objective of this evaluation was to determine the pathogenesis of the toxicity/toxicities and predictability from a nonclinical standpoint.

Methods and Materials: Publically available nonclinical and clinical data of compounds which have been discontinued as well as marketed compounds was evaluated.

Experimental Design: Sources of information included literature references and regulatory documents.

Results: Several of the compounds exhibited clinical evidence of mitochondrial toxicity, in particular those that resulted in the constellation of hepatic failure, pancreatitis and neuropathy. In other instances, the pathogenesis of the toxicity was considered to be related to mechanisms other than mitochondrial effects. *In vivo* nonclinical studies were often not predictive of the adverse clinical manifestations, irrespective of the suspected mechanism of the clinical toxicity.

Conclusion: The addition of *in vitro* testing to evaluate the potential for mitochondrial toxicity may provide valuable information for nucleoside/tide inhibitors. However, the final evidence for lack of clinical toxicity may depend upon human clinical evaluation (potentially into Phase 2 or Phase 3), particularly for those compounds for which the toxicity is associated with mechanism(s) other than mitochondrial toxicity.

Impact Statement: The development of nucleoside/tide inhibitors may result in unique challenges from a nonclinical and clinical perspective.

35

Graft-vs-Host Disease (GVHD) in NSG (NOD-SCID il2rγ-/-) Mice Engrafted with Human Hematopoietic Stem Cells (HSPCs)—Preclinical Findings and Clinical Relevance

Sundeep Chandra, Carlos Fonck, Valerie Ackley, Todd Oppeneer, Jill Woloszynek, Greg Hayes, Soumi Gupta, Charles O'Neill.
BioMarin Pharmaceutical Inc., San Rafael, CA, USA.

Autologous HSPCs have been used as targets of gene transfer, with applications in inherited disorders and cell therapy. NSG mice, lacking lymphocyte/NK cells are used to evaluate safety and efficacy of *ex vivo* modified human HSPCs. These "humanized" mouse protocols generally involve irradiation or chemical depletion of the murine hematopoietic compartment and transfer of human bone marrow, umbilical cord or peripheral blood-derived $CD34^+$ stem cells. Engrafted cells migrate to bone marrow and differentiate to all lineages of the mature immune system. GVHD observed in a 12-W NSG mouse study are presented here. Briefly, NSG mice were irradiated at the dose of 150 cGy and transplanted with naïve umbilical cord (UC) blood ($6.75x10^5$ cells), or with G-CSF mobilized peripheral blood HSPCs transduced with a mock vector encoding GFP or with a proprietary lentiviral vector encoding a modified human gene ($2.2X10^6$–$2.5X10^6$ cells). There were no microscopic findings in irradiated untreated mice or mice transplanted with UC blood. Almost all mice transplanted with naïve or transduced human HSPCs (GFP or lentiviral vector) had minimal to marked lympho-histiocytic inflammatory cell infiltrates consistent with GVHD primarily in the liver, lungs, spleen, or bone marrow with a few mice exhibiting similar infiltrates in the GIT and reproductive tissues. GVHD observed in NSG is due to donor T cells primed against murine antigens presented by graft-derived human cells, generating an immune response against murine host tissues. The murine findings, although not unexpected are unlikely to occur in human patients receiving "autologous" HSPCs.

36

Relationship between Teicoplanin-Induced Toxicity and Blood Concentrations in Neonates and Children

Takaaki Yamada, Satohiro Masuda.
Department of Pharmacy, Kyushu University Hospital, Fukuoka, Japan.

Introduction: Teicoplanin is an antibiotic used to treat methicillin-resistant *Staphylococcus aureus* infections in more than 60 countries. Although blood concentrations of teicoplanin should be ≥20 µg/mL for severe infections, nephrotoxicity and hepatotoxicity have been reported in adult patients. In this study, we examined the incidence of teicoplanin-induced nephrotoxicity and hepatotoxicity in neonates and children and evaluated the safety of teicoplanin with blood concentrations of ≥20 µg/mL.

Experimental Design: A total of 27 neonates and 86 children were treated with teicoplanin between October 2008 and March 2014.

Methods: During the period of teicoplanin administration, aspartate aminotransferase or alanine aminotransferase at >3× the upper limit of normal and serum creatinine at >1.5× baseline were defined as nephrotoxicity and hepatotoxicity. Teicoplanin blood concentrations were divided into <20 µg/mL and ≥20 µg/mL groups, and the incidence of nephrotoxicity and hepatotoxicity was compared.

Results: In neonates, the incidence of nephrotoxicity and hepatotoxicity was 20.0% and 14.8%, respectively. On the other hand, the incidence of nephrotoxicity and hepatotoxicity in children was 2.3% and 5.8%, respectively. In both cases, there was no significant difference in the incidence of the toxicities between <20 µg/mL and ≥20 µg/mL groups.

Conclusion: The risk of teicoplanin-induced toxicity is higher in neonates than in children. In addition, the incidence of nephrotoxicity and hepatotoxicity are independent of high blood concentrations.

Impact Statement: These results indicate that the target blood concentrations at ≥20 µg/mL for severe infections seem to be safe in neonates and children.

37

Spontaneous Hepatic Artery Degeneration/Necrosis in Young Male Sprague-Dawley Rats

Lily Yee, Tracy Carlson.
MPI Research, Mattawan, MI, USA.

Differentiating test article-related vascular changes from spontaneous background findings is important for microscopic interpretation. We observed a low incidence (up to 20% in individual studies) of spontaneous hepatic artery degeneration and necrosis in 3–9 month old control male Sprague-Dawley rats in routine safety studies. Two sections of liver, one from the median and one from the lateral liver lobe, were stained with hematoxylin and eosin and examined microscopically by board certified pathologists. The vascular degeneration was observed in one or two cross sections of medium-sized hepatic arteries near the hilus of the examined lobes. Microscopic changes ranged from acute intramural hemorrhage and fibrinoid necrosis to chronic fibrosis of the vascular wall and perivascular edema, hemorrhage, and infiltration of inflammatory cells. The cause of the change was uncertain. There were no other similar vascular changes in other tissues examined in these animals. It was not associated with changes in necropsy, trimming, or processing procedures and was not test article-related. Many microscopic features were consistent with polyarteritis or polyarteritis nodosa (PAN), however there was no similar change in arteries within tissues commonly affected in PAN (mesenteric, pancreatic, or testicular arteries) and it is unusual for young animals to present with PAN. This represents a possibly emerging background finding that may be confused with a toxicologic effect and should be carefully evaluated if seen.

38

Use of Telepathology for Pathology Peer Review in Multinational Studies

Gabe Siegel[1], Dan Regelman[1], Robert Maronpot[2], Moti Rosenstock[3], Abraham Nyska[4].
[1]*Augmentiqs, Misgav, Israel.* [2]*Maronpot Consulting, Raleigh, NC, USA.* [3]*Rosenstock Toxicologic Consulting, Haifa, Israel.* [4]*Tel Aviv University, Timrat, Israel.*

Introduction: Pathology peer review of toxicologic pathology findings in safety and efficacy assessment studies of new drugs is commonly done prior to submission of test results to regulatory authorities.

Experimental Design: Following completion of the pathology evaluation of a preclinical toxicity study at a contract laboratory in the United States, histopathology slides of renal tissue were shipped to the peer review pathologist (PR) located in Israel.

Methods: Using a regular microscope installed with a novel telepathology system (Augmentiqs™) (reference: Seigel et al), the PR was able to simultaneously share the actual histopathology slides with the study pathologist (SP), and obtain a consensus diagnosis for lesions in question. The SP was able to see the slides on his personal computer screen in high resolution, and discuss these lesions with the PR, while each side would make and view annotations and comments. All annotated projected microscopic fields were instantly photographed and saved by the PR pathologist.

Results: Following this live telepathology session and achieved consensus, the SP issued a revised report expressing the archived consensus diagnoses. Following completion of the entire peer review process and a more comprehensive onsite review of all organs, a formal GLP-compliant Peer Review Statement was signed by the SP and PR for regulatory submission.

Conclusion: Telepathology running off the microscope is a highly cost- and time-efficient method for conducting peer review with documented images.

Impact Statement: Based upon our experience, telepathology running off the microscope can be used for peer review and other GLP-compliant review applications.

39

Enabling Toxicologic Pathologists Using QuPATH, an Open Source Digital Pathology and Image Analysis Software Solution

Daniel Rudmann[1], Abigail Godbold[1], Maureen O'Brien[2], Brent Walling[1].
[1]*Charles River Laboratories, Ashland, OH, USA.* [2]*Charles River Laboratories, Frederick, MD, USA.*

Anatomic pathology is often a semi-quantitative science and assessing certain microscopic changes in preclinical studies can be laborious and prone to diagnostic drift. Computer-based image analysis (IA) could simplify numerous tasks common for the bench pathologist such as setting thresholds and establishing grading criteria for various tissue changes. Commercial IA solutions are available, but licenses are typically expensive and may limit use to a single computer or workstation. Historically, open source software image analysis solutions lacked the sophistication to tackle analyses using whole slide images (WSI). Recently, QuPath emerged as an alternative open-source platform for IA and aims to help improve the speed, objectivity and reproducibility of digital pathology analysis in WSI **https://qupath.github.io**. We developed algorithms in QuPath for 3 common diagnoses/measurements recorded in preclinical toxicology studies. QuPath was easily downloaded locally on computers, performed well on a variety of laptops and desktops, and did not require large storage space for analyses. Training pathologists required a modest time investment and a job aide was easily tailored from materials produced by QuPath developers. Numerous types of raw image files from different WSI scanners as well as conventional microscope cameras were dropped quickly into QuPath for analysis. The region of analysis (ROA) was simple to define using practical annotation tools. Algorithms were developed to evaluate the 3 diagnoses and preliminary data suggested they increased the diagnostic confidence and efficiency for the pathologists. We conclude that QuPath appears to have good potential as a tool for bench toxicologic pathologists.

40

Multiplexing Tyrosine Hydroxylase Immunohistochemistry and Luxol Fast Blue-Hematoxylin for Neuroanatomical Differentiation Using Stereology

Michael Staup, Danielle Brown, David Weil, Na Li, Jane Goad, Cynthia Swanson, Kyle Takayama.
Charles River Laboratories, Durham, NC, USA.

Introduction: Quantitative analysis within distinct anatomical areas of the brain following immunohistochemical (IHC) staining is difficult due to the challenge of creating regions of interest (ROIs) that accurately distinguish adjacent anatomical areas with similar antigen profiles. For example, the locus coeruleus (LC) and the subcoeruleus are continuous catecholamine-producing cell groups in the mouse midbrain. Fibers of passage can be used to precisely differentiate these areas.

Methods: Two series of physical disectors were collected at 50 µm intervals from the midbrain of four mice. Series 1 was stained for Tyrosine Hydroxylase (TH) against a hematoxylin counterstain. Series 2 utilized Luxol Fast Blue (LFB), a special stain used to identify myelinated fibers, as an additional counterstain.

Experimental Design: Four observers counted TH-positive cells within the LC from physical disectors using unbiased stereology. Observers counted cells within manually-generated ROIs from series 1, using a mouse brain atlas as a guide. The same methods were then applied to series 2 with ROIs created using fibers of passage on the LFB-stained sections.

Results: ROIs created using fibers of passage resulted in a decreased standard deviation for each mouse between observers. The statistical power of the sample size was also higher using the LFB-counterstain method.

Conclusion: Visualization of myelinated fibers of passage facilitates differential quantification of TH-positive cells in the LC from those in the subcoeruleus.

Impact Statement: Fibers of passage provide a rich source of information that can improve the precision of quantitative analysis in the brain through more consistent delineation of anatomical areas.

41

Quantitative versus Semiquantitative Assessment of Fibrosis in Unilateral Ureter Obstruction (UUO) Model in Mice

Jing Ying Ma[1], Bindu Bennet[2], Vinicius Carreira[1].
[1]*Pathology and Toxicology, Janssen Research & Development, LLC, San Diego, CA, USA.* [2]*Pathology and Toxicology, Janssen Research & Development, LLC, Spring House, PA, USA.*

Objectives: The objective of this study was to compare the assessment of fibrosis in Picrosirius Red (PSR) stained kidney sections through automated quantitative image analysis (IA) vs. the semi-quantitative evaluation as scored by a pathologist, and to compare fibrosis readouts between whole-kidney section versus cortico-medullary compartments in mouse unilateral ureteral obstruction (UUO) model studies.

Experimental Design: UUO surgeries were performed on a total of 80 male C57BL/6N-mice in 4 separate experiments (10/group). Mice were administered isotype control or TGFßmAb, at 10 mg/kg, i.p. every other day, starting 24 hours prior to surgery. All studies were terminated 10 days after surgery. Both kidneys were harvested, trimmed transversally at the level of the hilus, sectioned and stained with PSR. Renal fibrosis was semi-quantitatively evaluated by a pathologist and quantified by Visiopharm® software. Whole-kidney section and corticomedullary regions (without papilla and peri-pelvic stroma) were quantified separately.

Results: A statistically significant correlation ($p<0.0001$, $R^2=0.6$) between the semi-quanttative and quantitative analyses of PSR staining for fibrosis was observed in all four studies. TGFßmAb treatment resulted in a statistically significant decrease in fibrosis compared to the control, independent of evaluation of whole sections or corticomedullary only. Inclusion of the renal papilla and peri-pelvic stroma in the analyses resulted in higher standard deviation, and the differences between the mean of the two methods was statistically significant.

Conclusion and Impact Statement: High-throughput quantitative IA for renal fibrosis, adjusted for pre-analytical variables, represents a feasible, accurate, reproducible and efficient alternative to the semi-quantitative method.

42

Glomerular Identification and Quantification of Histological Phenotypes in the Mouse Using Image Analysis and Machine Learning

Susan Sheehan, Ron Korstanje.
The Jackson Laboratory, Bar Harbor, ME, USA.

Introduction: Current methods of assessing histological kidney samples, specifically glomeruli, do not allow for collection of quantitative data in a high-throughput and consistent manner. Rapid, comprehensive histological quantification could be used to significantly advance kidney research.

Experimental Design: Images of PAS stained mouse kidneys were used for training software to identify glomeruli. Validation was performed on images from additional mouse kidneys of different ages, strains, and sexes. Subsequently, this was integrated in an imaging workflow and used to compare mesangial matrix expansion (MME) scored manually and through automatic identification and quantification.

Methods: We used ilastik to train a classifier for glomerular identification and automatically route these to ImageJ for further analysis.

Results: Our classifier to identify glomeruli yields precision and recall rates of 98.4% and 95.2%, respectively. In our test case, we show significant correlation between glomeruli scored manually for MME and quantification using our automated workflow ($r^2 = 0.674$, $P < 5x10^{-8}$).

Conclusion: We developed a workflow for segmenting and analyzing glomeruli accessible to users without extensive histological or computational expertise (**https://github.com/TheJacksonLaboratory/Digital-Glomerular-identification**). The resulting data is free from user bias and continuous (such that statistical analysis can be performed), which allows for more precise and comprehensive interrogation of samples. This data can be combined with other physiological data to broaden our overall understanding of renal function.

Impact Statement: Image analysis represents an emerging field of untapped data, allowing for translational work across traditional disciplines. Improved methodology will allow investigators to extract more information from new and existing pathology slides.

43

Artificial Intelligence (AI)-Based Image Analysis and Decision Support System (iADSS) to Aid Pathologists in Analysis and Classification of Histopathology Images of WISTAR Rat Kidneys

Tijo Thomas, Uttara Joshi, Anindya Hajra.
Aditya Imaging Information Technologies, Thane West, India.

Introduction/Objectives: In recent years, Machine Learning techniques have helped in providing increasingly reliable and accurate solutions in Digital Pathology. iADSS combines advance algorithms of Image Processing with Deep Learning to Analyse and Classify Digital Histopathology Images from Pre-Clinical Toxicology studies. In this poster, we present iADSS results on Wistar Rat Kidneys vis-à-vis results of pathologist.

Methods and Materials: Kidney images were analysed and classified using Deep Learning models developed for normal tissue histology. Results were refined based on the observations [e.g., Basophilic Tubules, Dilated Tubules, Degeneration, Necrosis, Mononuclear cells (MNC), Polymorphonuclear Cells (pMNC), Hyperplasia or Shrunken Glomeruli in the segmented regions of Capsule, Cortex, Medulla and Papilla]. Trained models of *DeepLab* were used for segmentation of the Test data. Final classification was based structural and statistical properties of the detected parameters.

Experimental Design: Training was done using 500 images of 10 animals scanned at 40X. Test results were validated on 100 images and a separate case study on 119 animals was performed and validated by senior pathologists.

Results: On the case study, iADSS achieved an accuracy of 98.86% except one false-negative due to presence of a small focus of pMNC.

Conclusion: iADSS produced highly accurate and consistent analysis and classification of Rat Kidney images.

Impact Statement: iADSS can serve both as a decision support system and diagnostic tool in Digital Pathology in nonclinical toxicology studies.

44

A Robust *In Vivo* Model of Brain Metastases of Lung Cancer

Gozde Uzunalli, Alexandra Dieterly, Chinyere Kemet, Arvin Soepriatna, Aparna Shinde, Craig Goergen, Michael Wendt, L. Tiffany Lyle.
Purdue University, West Lafayette, IN, USA.

Introduction: Lung cancer remains one of the most common causes of brain metastases and cancer-related deaths. Non-small cell lung cancer (NSCLC) comprises the majority of cases. Treatment of NSCLC brain metastases is challenging; most current therapies are palliative. The therapeutic challenge is primarily attributed to the blood-brain barrier (BBB), which shifts in the presence of metastases to the blood-tumor barrier (BTB). To investigate the pathology and identify druggable targets of the BTB we developed a robust experimental model system.

Experimental Design: We developed a robust experimental model using brain-seeking adenocarcinoma NSCLC cells (A549-Br) to evaluate pathology and identify druggable targets.

Methods: An experimental model of brain metastases of NSCLC was developed using brain-seeking adenocarcinoma NSCLC cells (A549-Br) injected into the left cardiac ventricular lumen of 36 six-week-old athymic nude mice using ultrasound guidance.

Results: Brain metastases were evaluated over 1–6 weeks; a 3-fold increase in brain metastasis was present between 3 and 6 weeks. At 6 weeks, mice developed an average of 10 metastases. Interestingly, spinal cord metastases were present, causing paralysis. A striking variation in histologic features of neoplastic cells was observed within tissues and metastases.

Conclusion: This is the first comprehensive pathologic description of an *in vivo* model of brain metastases of NSCLC, adenocarcinoma subtype.

Impact Statement: The variation in histologic feature and epithelial to mesenchymal transition in our experimental model closely mirrors the pathology in patients and highlights the heterogeneity and associated treatment challenges of brain metastases of NSCLC.

45

Establishment of an *In Vitro* Hepatocarcinogenesis Model: Cell Proliferation of AML12 Cell Line Cultured in Presence of NNK

Andrea Midory Miyake, Marcia Kazumi Nagamine, Murilo Penteado Del-Grande, Nicolle Gilda de Queiroz Hazarbassanov, Cristina de Oliveira Massoco de Salles Gomes, Ivone Izabel Mackowiak da Fonseca, Maria Lucia Zaidan Dagli.
Universidade de São Paulo, São Paulo, Brazil.

Introduction: Hepatic neoplasias are increasingly prevalent and preventive or therapeutic approaches are necessary. Many *in vivo* models of hepatocarcinogenesis are available; however, they are expensive and request the use of many animals. Therefore, the development of *in vitro* models for these neoplasias becomes essential to understand the molecular alterations associated with the carcinogenesis process, and their control. This study aims to establish an *in vitro* model of hepatocarcinogenesis with 4-(methylnitrosamino)-1-(3-pyridyl)-1-butanone(NNK). Here we present the cell growth rate during *in vitro* culture.

Experimental Design: normal hepatocyte cell line derived from mice (AML 12, Mus musculus, CRL-2254) was cultured in the presence of carcinogenic agent NNK. The experiment was divided into three groups: treatment group, which was submitted to 30 cycles of carcinogen exposure; negative control group, and positive control group constituted by HEPG2 cells.

Methods: Three independent experiments were performed in triplicate. Cell proliferation capability was measured by analysis of cell cycle using propidium iodine staining and flow cytometry.

Results: Treatment group showed a higher percentage (10,42% + 7,709; $p<0,05$) of cells in S phase of the cell cycle than negative control group (2,49% + 0,8502).

Conclusion: These results indicate NNK carcinogen was capable of increasing the growth rate of normal hepatocytes after 30 cycles exposure.

Impact Statement: The *in vitro* model has been established and further characteristics of this model are under study.

46

Toxicogenomics Study of Pentabrominated Diphenyl Ethers (DE-71 Mixture and Its Congener PBDE-47) in Rat Liver after Early Life Exposure

Arun Pandiri[1], Keith Shockley[1], Dan Morgan[1], Grace Kissling[1], Thai-Vu Ton[1], Ralph Wilson[1], Sukhdev Brar[1], Amy Brix[2], June Dunnick[1].
[1]*National Institute of Environmental Health Sciences, Research Triangle Park, NC, USA.* [2]*Experimental Pathology Laboratories, Inc, Research Triangle Park, NC, USA.*

Introduction: Pentabrominated diphenyl ether (PBDEs) flame retardants used in polyester foams and other household products have led to widespread human exposure in the United States. Early-life exposure to PBDEs has been associated with loss of Intelligence Quotient (IQ) and altered serum thyroxine (T_4) levels in humans. A PBDE mixture (DE-71) caused hepatocellular tumors in Wistar Han rats and B6C3F1/N mice in an NTP 2-year bioassay. In humans the most prevalent PBDE congener is PBDE-47 and it has no safety information.

Experimental design: We have characterized the toxicity and transcriptomic profiles of DE-71 mixture and its congener PBDE-47 in PND22 in Wistar Han rat pups after *in utero*/postnatal gavage exposure (0, 0.1, 15, or 50 mg/kg; dams GD6-21/pups PND12-21).

Results: Both DE-71 and PBDE-47 induced hepatic fatty change and reduced T_4 levels. Hepatic transcriptomic profiling demonstrated 231 and 593 altered genes (FDR 5%) in DE-71 and PBDE-47 (both at 50 mg/kg) compared to control livers, respectively. The altered molecular pathways in both datasets were comparable and included alterations in cytochrome p450 enzymes, Nrf2-mediated oxidative stress response and ABC transporters.

Impact Statement: After early life exposures, both DE-71 and PBDE-47 had similar morphologic lesions, similar reductions in serum T_4 levels and similar alterations in molecular pathways, and it is likely that PBDE-47 congener might also be a rodent liver carcinogen after continued long-term exposure similar to the PBDE mixture DE-71 (National Toxicology Program 2017, Technical Report 589).

47

Fibrosarcoma with Unique Histomorphologic Features in the Small Intestine of Wistar Han Rats in a Two-Year Carcinogenicity Study

Kiran Palyada, Thomas Forest, Christine Reichard, Caron Leach, Takayuki Tsuchiya.
Merck and Company, West Point, PA, USA.

Introduction: Mesenchymal tumors are relatively uncommon as a spontaneous or background finding in the gastrointestinal tract of rodents in carcinogenicity studies. In this report, we characterize two tumors in the wall of the jejunum of rats in 2-year carcinogenicity study.

Experimental Design: Wistar Han rats were given daily oral doses of 4 control articles-(0.5% [w/v] methylcellulose in deionized water, hydroxypropyl methylcellulose acetate succinate [HPMCAS], 10% [w/w] polysorbate 80 in deionized water, or 100% polyethylene glycol 400) for approximately 2 years.

Methods: The small intestines were fixed, sectioned and stained with H&E and trichrome. Additional sections of the intestine were immunostained with primary antibodies against cytokeratin, vimentin, smooth muscle actin, CD117, CD34, or S-100.

Results: The neoplastic cells expanded, obscured or obliterated the inner and outer muscular layers of the jejunum and formed a grossly visible nodule in one rat. The neoplasm lacked classical features of a mesenchymal tumor with neoplastic cells arranged in sheets with ovoid to irregular nuclei and scattered mitotic figures. The neoplastic cells in both tumors were positive for vimentin and negative for pan-cytokeratin, smooth muscle actin, S-100, and CD117. The stroma in both tumors was positive for trichrome indicating the production of collagen by the neoplastic cells. A subset of neoplastic cells was positive for CD34 in one tumor while the other tumor was negative for CD34.

Conclusion: Based on the results of immunohistochemistry, these tumors were diagnosed as fibrosarcomas.

48

Mitochondrial Genomic Alterations in Spontaneous and Chemical-Induced Hepatocellular Carcinomas in B6C3F1/N Mice

Miaofei Xu[1], Adam Burkholder[2], David Fargo[2], Jacqui Marzec[3], Steven Kleeberger[3], Gregory Solomon[4], Robert Sills[1], Arun Pandiri[1].
[1]*Division of National Toxicology Program (DNTP), NIEHS, Research Triangle Park, NC, USA.* [2]*Center for Integrative Bioinformatics, NIEHS, Research Triangle Park, NC, USA.* [3]*Immunity, Inflammation, and Diseases Laboratory, NIEHS, Research Triangle Park, NC, USA.* [4]*Epigenemoic Core, NIEHS, Research Triangle Park, NC, USA.*

Introduction: Mitochondria play an important role in cellular energy metabolism. Under xenobiotic stress, free radical generation and subsequent chronic oxidative stress have been implicated in many carcinogenic processes.

Experimental Design and Methods: We hypothesized that chronic oxidative stress and secondary mitochondrial alterations could contribute to chemical induced carcinogenesis. We performed ultra-deep (50,000x) whole mitochondrial DNA (mtDNA) sequencing and mtDNA copy number analysis on fresh-frozen B6C3F1/N mouse hepatocellular carcinomas (HCCs) that arose either spontaneously (n=20, 10/sex) or due to 2-year exposure to a genotoxic carcinogen, gingko biloba extract (GBE; n=10, male only) and a non-genotoxic carcinogen, anthraquinone (n=10, male only); age-matched non-tumor controls (n=20, 10/sex) were also included.

Results: In total, 958 mtDNA mutations sites were detected. Of those, the number of non-synonymous mutations in the GBE-induced HCCs (n=790) was extremely high compared to anthraquinone-induced (n=258) or spontaneous (n=290) HCCs. Mutation signature analysis demonstrated predominantly G/C to T/A transversions in GBE-induced HCCs, suggesting 8-oxo-guanine adduct formation secondary to oxidative stress. The mtDNA copy number analysis revealed a significant reduction in spontaneous (p=0.006) and anthraquinone-induced (p=0.001) HCCs but not in GBE-induced HCCs (p=0.4).

Conclusion: Alterations in mtDNA genome indicated that GBE likely has a genotoxic mode of action and anthraquinone, a non-genotoxic mode of action.

Impact Statement: To our knowledge, this is the first study to demonstrate distinct mtDNA alterations in spontaneous and chemical-induced HCCs. Unique mtDNA mutation spectra and copy number variation could help us better understand the mode of action in chemical carcinogenesis.

49

Preclinical Activity of Tipifarnib in Cutaneous T-Cell Lymphoma

Rebecca Kohnken[1], Betina McNeil[1], Jing Wen[1], Kathleen McConnell[1], Basem William[1], Francis Burrows[2], Pierluigi Porcu[3], Anjali Mishra[1].
[1]*Ohio State University, Columbus, OH, USA.* [2]*Kura Oncology, San Diego, CA, USA.* [3]*Thomas Jefferson University, Philadelphia, PA, USA.*

Introduction: Cutaneous T-cell lymphoma (CTCL) is a rare form of non-Hodgkin lymphoma characterized by malignant infiltration of skin-homing CD4+ T-cells, manifesting clinically as patches and plaques on the skin. Farnesyl transferase inhibitors (FTIs) are a relatively new class of anticancer drugs, the exact mechanism of which is unknown. Tipifarnib is one such FTI, which has demonstrated clinical activity as a single agent in patients with relapsed and refractory lymphomas.

Experimental Design: Tipifarnib efficacy was evaluated *in vitro* utilizing five CTCL patient-derived cell lines. Interleukin (IL)-15 transgenic mice were used as a model of CTCL to determine the *in vivo* efficacy of tipifarnib.

Methods: Cell viability was measured by MTS assay, and apoptosis was evaluated by flow cytometry. 5-week-old IL-15 transgenic mice were treated with 100 mg/kg tipifarnib, or vehicle control, by oral gavage twice a day for 2 weeks. Following sacrifice, skin was collected in 10% neutral buffered formalin, processed, sectioned, and stained (hematoxylin and eosin). Gross and histologic lesion severity evaluation was performed.

Results: Tipifarnib resulted in dose-dependent decreases in cellular viability in CTCL patient-derived cell lines. This finding correlated with an increase in apoptotic cell death. *In vivo*, tipifarnib treated mice had significantly reduced gross and histologic lesions of CTCL as compared to vehicle-treated mice.

Conclusion: Tipifarnib is active in early preclinical models of CTCL.

Impact Statement: Based on these data, further studies to elucidate the mechanisms of antitumor activity of farnesyl transferase inhibition in T-cells are warranted.

50

Toxicity and Toxicokinetic Study of Subcutaneously Administered RPh201 in Minipigs

Yuval Ramot[1], Zadik Hazan[2], Andre Lucassen[2], Konstantin Adamsky[2], Vanessa Ross[3], Nigel Young[3], Abraham Nyska[4].
[1]*Hadadssah-Hebrew University Medical Center, Jerusalem, Israel.* [2]*Regenera Pharma, Nes-Ziona, Israel.* [3]*Envigo, Ltd., Alconbury, Cambridgeshire, United Kingdom.* [4]*Consultant in Toxicologic Pathology, Timrat, Israel.*

Introduction: Mastic gum extracts have been traditionally used as a dietary additive and as a flavouring agent. They are being tested for many clinical indications. Nevertheless, the safety profile of these extracts is still not entirely elucidated. RPh201 is an extract of the mastic gum, formulated and stabilized in a proprietary method, which is being developed for a wide range of neurological indications. Our aim was to test the safety and toxicokinetic profile of RPh201 administered SC for 9 months.

Experimental Design: 32 male and 32 female Göttingen minipigs were administered subcutaneous injections of RPh201 (0, 3.1, 12.5.50 mg/kg) twice weekly for 39 weeks. There was a 26-week interim phase and a 6-week recovery period.

Results: RPh201 was well tolerated for 39 weeks with no clinical or dose-related signs observed. Treatment-related findings were seen at the injection sites of the high-dose animals, which included abscesses, chronic inflammation and subcutaneous fibrosis. There was partial recovery from both the abscess formation and fibrosis. In addition, cystic spaces were found in the subcutaneous injection sites and in the lymph nodes, kidney and lungs, resulting from accumulation of the vehicle (cottonseed oil) at large amounts. These findings were considered not to be adverse.

Conclusion: Doses up to 50 mg/kg of RPh201 were well tolerated in Göttingen minipigs for 39 weeks of administration, and the NOAEL was 12.5 mg/kg/injection.

Impact Statement: RPh201 is a promising new and safe drug candidate for the treatment of several neurological indications.

51

Inhaled Furan Selectively Damages Club Cells in Lungs of A/J Mice

Alexandru-Flaviu Tabaran[1,2], Lisa A. Peterson[3], M. Gerard O'Sullivan[1,2].
[1]*College of Veterinary Medicine, University of Minnesota, Saint Paul, MN, USA.* [2]*Comparative Pathology Shared Resource, Masonic Cancer Center, University of Minnesota, Saint Paul, MN, USA.* [3]*Division of Environmental Health Sciences, Masonic Cancer Center, University of Minnesota, Minneapolis, MN, USA.*

Introduction/Objectives: Furan is a volatile organic compound that is a product of incomplete combustion, and is present in cigarette smoke, engine exhaust, and processed food. Oral administration of furan induces liver tumors in F344 rats and B6C3F1 mice, and it is classified as a possible human carcinogen. Furan-induced toxicity following air exposure has not been well characterized.

Experimental Design/Materials and Methods: A/J Mice (n=2/group) were nose-only exposed for 3 h to furan (0, 30, 75, 150, 300 or 600 ppm) and euthanized at 24 h, 48 h, or 1 week. Histopathology evaluation of major organs including lung was performed.

Results: Exposure to 300 and 600 ppm furan for 3 hours caused bronchiolar club cell necrosis (diffuse, marked) with airway denudation, and with partial recovery (regeneration of epithelium) at 1 week post-exposure. The 3 hour exposure caused mild damage (150 ppm) or acute centrilobular necrosis and mineralization in livers (300 and 600 ppm). Recovery was present by 1 week, with the exception of the 300 ppm group which there had multifocal mineralization that evoked a mild granulomatous response.

Conclusion: Furan is toxic to lungs and liver when inhaled.

Impact Statement: Inhaled furan is toxic to lung and liver, with club cells being the target cell in lung. Club cell toxicity likely relates to bioactivation of furan by club cell cytochrome P450 2E1 to 2-*cis*-butene-1,4-dial, a known mechanism of toxicity for furan.

52

Infusion Procedure-Related Pathology of Intravenous Catheterized Rats

Amit Kumar[1,2], David Rehagen[2].
[1]*Michigan State University, Lansing, MI, USA.* [2]MPI Research, Mattawan, *MI, USA.*

Introduction: Intravenous infusion is a common route of drug delivery for investigational drug administration. During infusion studies, catheter- and procedure-related vascular lesions may occur, which can confound interpretation. Hence, it is important to differentiate these from test article effects. This study presents background microscopic lesions observed at the infusion site in a rat model using INHAND nomenclature.

Experimental Design: A total of 90 Sprague-Dawley rats (45 male and 45 female) with surgically implanted catheters were administered saline solution via 24-hour continuous infusion and necropsied on Days 29, 57, and 85 (30 rats per interval). The infusion site and surrounding tissues were fixed in 10% formalin. H&E stained slides of the vessel and surrounding tissues proximal to, distal to, and at the catheter tip were examined.

Results: The most common microscopic findings were thrombus and intimal proliferation. Degeneration/necrosis of the vascular wall, hemorrhage, and perivascular/vascular inflammation were also common. INHAND terminology was generally applicable for the majority of infusion-related findings.

Conclusion: A range of procedure-related lesions frequently occur at the infusion site and may confound the interpretation of test article-related findings.

Impact Statement: Current INHAND terminology can be used to characterize the majority of procedure-related findings at infusion sites; however, further discussion of background lesions at infusion sites is warranted to guide diagnosis and documentation of findings for regulatory (SEND) submissions.

53

Characterization of a Novel Pulmonary Arteriopathy in Control Beagle Dogs

Juliane Daggett[1], Keith Nelson[2], James Reindel[2].
Midwestern University, College of Veterinary Medicine, Glendale, AZ, USA. [2]MPI Research, Mattawan, MI, USA.

Beagle dogs used in toxicology studies have various well-defined background pulmonary parenchymal changes, but pulmonary vascular changes have not been amongst these findings. We identified a pulmonary hypertrophic arteriopathy (HA) in beagles enrolled in safety studies and conducted a review of control dogs to further characterize the nature and incidence of this change. Routine sections of apical and diaphragmatic lung lobe from 239 control dogs (116 females, 123 males) from safety studies from 2015 to 2017 were examined for changes consistent with HA. Seven of 239 dogs (2.9%) had HA characterized as pronounced multifocal thickening of pulmonary arteries (PAs) of variable caliber, including the intima and/or media of affected vessels. Normal and abnormal PAs occurred in the same lung section. HA occurred in both sexes, was limited to the diaphragmatic lobe, and occurred in oral and intravenous studies. The intima of many affected vessels had infiltrates of fibromuscular stromal cells. Vascular luminal recanulization and foci of adventitial neovascular proliferation were present in some artery sections, but thrombi were not observed. The media of many affected vessels were substantially thickened by hypertrophic and hyperplastic smooth muscle cells. Basophilia of medial myocytes and fibromuscular intimal cells and hemosiderin in perivascular tissue occurred in some vessels, indicating ongoing vascular remodeling. Inflammatory infiltrates were not a major component of the change. The etiology of this localized arteriopathy is unknown. Establishing this as a background change in controls helps to reduce the misinterpretation of the importance of this change occasionally seen in treated dogs.

54

Proposed Mode of Action for Uterine Adenocarcinomas in Han Wistar Rats Treated with Isopyrazam (IZM)

Jayne Wright[1], Elizabeth McInnes[2], Sue Yi[2], Richard Peffer[3], David Cowie[2], Paul Parsons[4], Richard Currie[2], Ryan Richards-Doran[2], Douglas Wolf[3], Kristin Lichti-Kaiser[3].
[1]Syngenta Consultant, Bracknell, United Kingdom. [2]Syngenta, Bracknell, United Kingdom. [3]Syngenta, Greensboro, NC, USA. [4]Exponent, Liverpool, United Kingdom.

Introduction: In a 2-year carcinogenicity study, rats exposed to 232.8 mg/kg/day IZM resulted in a significant increase in uterine adenocarcinomas and a decrease in mammary fibroadenomas and pituitary adenomas. Concomitantly, there was also a significant, severe reduction in body weight gain (30–40%). It was hypothesized that the treatment related tumors may reflect altered or delayed reproductive senescence.

Experimental Design: Female Han Wistar Crl: WI(Han), 145 rats/grp, were dosed with 500 and 3000 ppm IZM and compared to untreated control group.

Methods: The estrous cycle was monitored at 2–3 week intervals (daily vaginal lavage) throughout the study. Blood samples for hormone evaluation were collected. Uterus, ovaries, vagina and pituitary were examined microscopically.

Results: Test substance-related lower fat pad weights, higher liver weights and reduced body weight gain were observed in the 3000 ppm IZM in particular. Estrous cycle data indicated that rats treated with 3000 ppm of IZM continued to cycle regularly for a longer period of time than the control rats. Mean prolactin and leptin levels were lower in 3000 ppm IZM treated rats.

Conclusions: Uterine adenocarcinomas observed female rats for 3000 ppm IZM group in a 2-year carcinogenicity study were likely due to differences in the pattern of transition into reproductive senescence.

Impact Statement: The results of this study as well as physiological differences in control of the reproductive cycle and the transition in to reproductive senescence between rats and humans demonstrate that this MoA is not relevant to humans.

55

An Immunohistochemical Investigation of TGFß Receptor-1 Inhibitor-Induced Renal Epithelial Proliferative Lesions in Cynomolgus Monkeys

Jing Ying Ma, Sandra Snook, Vinicius Carreira.
Preclinical Development & Safety, Janssen Research & Development, LLC, San Diego, CA, USA.

Objectives: To use immunohistochemistry (IHC) to confirm and refine the diagnosis of test article-related renal proliferative epithelial lesions in a 21-day toxicity study in monkeys.

Experimental Design: Formalin-fixed, paraffin-embedded sections from the kidney of control and high-dose TGFßR1 inhibitor-treated monkeys (n=3/gender/group) were immunostained and evaluated for the expression of Vimentin, CK19, α-SMA, Factor VIII, and PCNA, plus routine hematoxylin and eosin (H&E) stain.

Results: In the control kidney, vimentin expression was restricted to the vessels, interstitium, glomerular tuft, Bowman's epithelium, and distal-most portion of the papillary collecting ducts. CK19 was intensely expressed from the distal convoluted tubules to collecting tubules and urothelium. Proliferative nodular epithelial lesions, present in the pelvic region of 2/6 monkeys in the high-dose group were both CK19 positive, but α-SMA and FVIII negative. Vimentin was diffusely positive in one tumor and in the dilated cortical tubules of the same kidney, as well as multifocally positive in cells at the base of the other tumor. Increased proliferation was evidenced by abundant PCNA positive nuclei in the two tumors and throughout cortical and medullary tubules in the treated group. Epithelial neoplastic embolization was confirmed by luminal CK19 and vimentin positive cells within FVIII positive vascular profiles. α-SMA staining highlighted invasion of the sub-urothelial muscular layer.

Conclusion: IHC findings corroborated the diagnosis of carcinoma arising from the urothelium and/or papillary distal collecting ducts.

Impact Statement: Ancillary techniques are invaluable tools to confirm and refine challenging diagnoses, such as atypical proliferations arising in unusual contexts.

56

GPER-Dependent Transactivation of EGFR Is Required for Human Leiomyoma Cell Proliferation Induced by Cadmium (Cd): A Nongenomic Mechanism for Cd's "Metalloestrogenic" Effects

Jingli Liu, Linda Yu, Lysandra Castro, Yitang Yan, Alanna Burwell, Darlene Dixon.
Molecular Pathogenesis Group, National Toxicology Program (NTP) Laboratory, NTP, National Institute of Environmental Health Sciences, National Institutes of Health, Research Triangle Park, NC, USA.

Introduction: Cadmium (Cd) is an environmental contaminant implicated as a "metalloestrogen." Uterine leiomyomas (fibroids) are estrogen-responsive gynecologic neoplasms affecting nearly 70% of reproductive-aged women. We have shown that Cd stimulates human uterine leiomyoma (ht-UtLM) cell proliferation through EGFR/MAPK activation, but not by classical estrogen receptor (ER) binding. Whether nongenomic ERs (GPER, ERαSer118, or ERα36) are involved is unknown.

Experimental Design: Human fibroids and patient-matched myometrial tissues were evaluated for GPER and phospho-EGFR expression. Signaling pathways were assessed in ht-UtLM cells exposed to Cd (0.1 or 10 μM), E_2, or G1 (GPER-specific agonist) for 10 min, or 24, 48, 72 h; with or without G15 (GPER-specific antagonist) pretreatment, or silencing (si) of GPER, or ERα36.

Methods: Protein expression/activation, cell proliferation, and signaling pathways were evaluated by western blotting, cell counting kit-8 assays, flow cytometry, immunofluorescence, and zymography.

Results: Phospho-EGFR and GPER were highly expressed in fibroids compared to myometrial tissues. At 48 h, Cd increased GPER expression and proliferation in ht-UtLM cells that was inhibited by G15 and siGPER, but not by siERα36. Cd-activated MAPK was dependent on GPER/EGFR transactivation, through significantly increased phospho-Src, matrix metalloproteinase-2 (MMP2)/MMP9, and HB-EGF expression/activation. Cd did not induce ERαSer118 activation.

Conclusions: Cd induced ht-UtLM cell proliferation through GPER/p-Src/MMP2/MMP9/HB-EGF/EGFR/MAPK nongenomic signaling, but not by ERα36 or ERα-phospho-Ser118 pathways.

Impact Statement: Cd may be a risk factor for women with fibroids, and crosstalk between hormone and growth factor pathways are involved in Cd-induced signaling.

57

Pancreatic Effects of Valosin-Containing Protein (VCP) Inhibition in Mice and Rats

Karyn Enos, Francis Wolenski, James Gavin, Sean Harrison, Allison Berger, Sandy Gould, William Mallender.
Takeda Pharmaceuticals International Co., Cambridge, MA, USA.

Introduction: Valosin-containing protein (VCP) is an essential enzyme that works to extract misfolded proteins from the endoplasmic reticulum, and is critical for protein homeostasis. VCP-inhib is a novel, irreversible VCP small molecule inhibitor that was evaluated for efficacy against multiple myeloma xenografts in immunocompromised mice and toxicity in rats.

Experimental Design: In study #1, female SCID mice (7/group) were implanted subcutaneously with MM1S tumor cells and dosed with VCP-inhib (0.1mg/kg twice weekly intravenously) beginning 2 weeks later. In study #2, naïve male Sprague-Dawley rats (4/group) were dosed intravenously (0.1 mg/kg once weekly).

Materials and Methods: For study #1, limited clinical and anatomic pathology including blood glucose and microscopic examination of the pancreas, liver, and kidneys was performed. For study #2, full clinical pathology as well as microscopic examination of adrenal glands, liver, pancreas, pituitary, prostate, thyroid, parathyroid and mandibular salivary gland were performed.

Results: Both studies were terminated early due to body weight loss. In mice, clinical chemistry revealed hyperglycemia and histopathologic examination of the pancreas revealed degeneration and necrosis of pancreatic islet cells. In rats, VCP-inhib related microscopic changes included atrophy of the exocrine pancreas with degeneration, necrosis, and mitotic figures of acinar cells.

Conclusion: Administration of VCP-inhib to mice and rats was not tolerated at 0.1 mg/kg (twice weekly or weekly, respectively) and induced pancreatic toxicity.

Impact Statement: VCP-inhib-related pancreatic toxicity was dramatically different between mouse and rat which may be related to species differences in VCP distribution, function, or metabolism.

58

Renal Lesions Associated with Soy-Deficient Diet in Rats

Catherine Picut[1], Eli Parker[1], Stephanie White-Hunt[1], Kathleen Szabo[2], Jessica Keen[3], Pragati Coder[3], Pallavi McElroy[3].
[1]*Charles River Laboratories, Durham, NC, USA.* [2]*Charles River Laboratories, Frederick, MD, USA.* [3]*Charles River Laboratories, Ashland, OH, USA.*

Introduction/Objectives: PMI Nutrition Rodent LabDiet® 5K96 is a natural ingredient diet low in soy isoflavones. It is recommended for use on developmental and reproductive toxicity (DART) studies, especially those designed to detect endocrine disruptors. The objective of this study was to determine the incidences and severities of 5K96-associated renal lesions in control rats.

Experimental Design/Methods: Kidneys from control animals (F_0 and F_1 generations) from four multigenerational DART studies, employing 5K96 diet, were evaluated microscopically. Tissue sections were stained by H&E, von kossa, and alizarin red. The incidence and severity of renal findings were compared to historical control (HC) database of age-matched rats fed traditional diets (LabDiet® 5002).

Results: Nephrocalcinosis and/or nephropathy were present in higher incidences and severities in females compared to historical controls. The incidences/average severities of nephrocalcinosis were up to 93%/1.6 (F_0) and 100%/3.3 (F_1) females; and of nephropathy up to 91%/1.85 (F_1) females.

Conclusions: The 5K96 diet resulted in relatively high incidence and severity of renal mineralization and/or nephropathy in control females in both F_0 and F_1 cohorts, with F_1 females being affected to a greater degree.

Impact Statement: The lesions in kidneys of control female rats fed 5K96 diet may increase vulnerability of the kidney to possible test article (TA)-related effects, especially in the F_1 cohorts. Caution should therefore be used when interpreting, or determining risk of, a TA-related effect in the kidney for studies using a low soy isoflavone diet.

59

Histologic Background Findings of the Lung in Beagle Dogs: A Comparison between Apical and Diaphragmatic Lobes

Juliane Daggett[1], James Reindel[2], Keith Nelson[2].
[1]*Midwestern University, College of Veterinary Medicine, Glendale, AZ, USA.*
[2]*MPI Research, Mattawan, MI, USA.*

Introduction: Beagles are the most common non-rodent model used in toxicology studies and evaluation of background findings is valuable in assessing potential test article effects. Aims of this study include retrospective characterization of background histologic findings in control beagles, and categorizing apical versus diaphragmatic lobe distribution of the findings.

Methods: Lung slides from 239 control beagle dogs (116 females, 123 males) used in 33 toxicology studies from 2015 to 2017 were evaluated by the authors. Hematoxylin and eosin-stained slides of the apical and diaphragmatic lung lobes were assessed for all animals, noting findings within each lobe separately. Severity was assessed using a 4-step grading system.

Results: The majority of the histologic changes consisted of variable types of inflammation. The most commonly seen finding was mononuclear cell infiltration within alveolar walls, followed by eosinophilic debris in the alveolar space. The apical lobe (56.1%) was more commonly affected overall than the diaphragmatic lobe (38.9%).

Conclusion: The most common findings consisted of minor chronic inflammation that was not associated with clinical signs. Background findings are more commonly seen in the apical lobe versus the diaphragmatic, although both lobes may have findings.

Impact Statement: This assay of pulmonary background findings provides valuable information about the incidence, severity, and anatomic location of histologic findings that are not associated with test article administration in purpose-bred beagle dogs. Additionally, there is a benefit in assessing multiple lung lobes.

60

Effect of Combined Dyslipidemia and Hyperglycemia on Diabetic Peripheral Neuropathy in Alloxan-Induced Diabetic WBN/Kob Rats

Kiyokazu Ozaki, Tetsuro Matsuura.
Setsunan University, Osaka, Japan.

Introduction: Clinical and experimental research has suggested that dyslipidemia aggravates diabetic peripheral neuropathy (DPN). However, whether dyslipidemia is a risk factor for DPN remains unclear. To investigate the effect of dyslipidemia on DPN, morphological features of peripheral nerves were analyzed in diabetic rats treated with a high-fat diet (HFD).

Experimental Design and Method: Male rats were divided into four groups: nondiabetic rats with standard diet (N group), nondiabetic rats treated with an HFD (HF group), alloxan-induced diabetic rats with standard diet (AL group), and diabetic rats treated with an HFD (AH group). Rats received HFD or standard diet from 13 weeks of age, and were sacrificed at 36 weeks of age.

Results: Combined hyperglycemia and dyslipidemia (AH group) induced a significant increase in plasma triglyceride and cholesterol levels. In addition, the combined effects contributed to a reduction in myelin size and a reduction in myelin thickness as indicated on sensory sural nerve histograms. There was also a reduction in the size of motor nerve axons when compared with the effects of hyperglycemia or dyslipidemia alone. However, the sensory nerve conduction velocity in the AH group was slightly but not significantly lower than those in the HF and AL groups.

Conclusion: These results suggest that combined hyperglycemia and dyslipidemia may induce mild peripheral motor and sensory nerve lesions, without significantly affecting sensory nerve conduction velocity.

Impact Statement: Dyslipidemia may injure peripheral motor and sensory nerve of diabetic rat.

61

Glomerulosclerosis and Dysplasia of Medulla, Gentamicin-Induced Unique Nephrotoxicity in Juvenile Rats

Kiyonori Kai, Kumi Honda, Kyohei Yasuno, Shinobu Hakamata, Kazunori Fujimoto, Noriyo Niino, Kazuhiko Mori.
Daiichi Sankyo Co., Ltd., Tokyo, Japan.

Introduction: Kidney development in rats extremely is different from human, and nephrotoxicity profile in juvenile rats differs from that of matured rats caused by renin-angiotensin system modulation drugs. Gentamicin is chosen as a compound that induces proximal tubular lesions, and the feature of nephrotoxicty and its recovery were evaluated in juvenile rats.

Materials and Methods: Gentamicin (30 mg/kg) was subcutaneously injected to male Sprague-Dawley rats from the day after the delivery for 20 days.

Experimental Design: Urinalysis, blood biochemistry, measurement of angiotensinogen in serum and urine, and pathological examination and toxicogenomics were performed on day of the recovery 1, 9, 16, and 30.

Results: On the recovery Day 1, serum UN and CRE were increased. Histopathologically, necrosis of proximal tubular epithelium accompanied with regeneration of tubular epithelium, dilatation of tubule, fibrosis of interstitium and dysplasia of medulla were noted. Glomerulosclerosis was observed, and phosphorated Stat 3 and a-SMA positive cells were immunohistochemically identified. Angiotensinogen, albumin, Kim-1, osteopontin and NGAL were increased; angiotensinogen and albumin tended to be raised in the latter recovery period. On the recovery day 9, necrosis of proximal tubular epithelium were recovered, but glomerulosclerosis was worsened associated with the increase in PAM positive fiber. In the gene expression analysis, common feature both in the cortex and medulla were increased expression of TGF-b1-related genes.

Conclusions: Gentamicin, well-known nephrotoxic agent of proximal tubular epithelium in mature rats induced glomerulosclerosis and dysplasia of the medulla in juvenile rats.

Impact Statement: Gentamicin revealed unique nephrotoxicity in juvenile rats.

62

Adverse Effect of Intra-Arterial Carboplatin Chemotherapy for Retinoblastoma in a Rabbit Model

Lauren Himmel, Tai Oatess, Kelli Boyd, Anthony B. Daniels.
Vanderbilt University Medical Center, Nashville, TN, USA.

Introduction: Intra-arterial chemotherapy (IAC) is emerging as a powerful tool for retinoblastoma, but is associated with local ocular toxicities. We used a rabbit model to explore response to IAC.

Experimental Design: Non-xenografted 3.0 kg male New Zealand White rabbits received endovascular microcatheter infusions of carboplatin. Over 2 separate experimental cohorts, 10/12 (83%) eyes from 6 animals treated unilaterally developed severe uni- or bilateral periocular edema; 1 cohort (n=3, 50 mg) developed edema immediately postoperatively necessitating euthanasia and 1 cohort (n=3, 25 mg) developed edema approximately 24 hours postoperatively, with 2 being euthanized upon becoming symptomatic and 1 being medically managed for 4 days until it was euthanized for intractable edema-related lagophthalmos.

Methods: Globes and orbits from all 6 euthanized rabbits were harvested *en bloc* and whole mount sections were prepared and stained with H&E for histologic evaluation.

Results: Histopathology demonstrated a time-course progression in light microscopic lesions, with edema and early heterophilic infiltrates being present in rabbits euthanized upon developing symptoms, progressing to fibrin exudation, thrombosis, and coagulation necrosis in more mature lesions.

Conclusion: The main underlying pathogenesis of carboplatin-associated toxicity in these cases appears to be vasogenic edema in confined spaces, perpetuating circulatory compromise and tissue ischemia.

Impact: It was assumed that melphalan, which causes vascular toxicity as a single agent, was the prime cause of the often-seen periorbital edema in patients receiving combination IAC for retinoblastoma; however, these experiments suggest that carboplatin may be an important cause. Species-specific anatomic features of lagomorphs could also contribute to complications of ocular IAC.

63

Dapagliflozin Does Not Act as a Tumor Promoter or Progressor in a Rodent Model of Urothelial Bladder Cancer

Magnus Söderberg[1], Agathe Bédard[2], Solomon Haile[2], Bassem Attalla[2], Jason Kirk[3], Martin Billger[4].

[1]*Pathology, Drug Safety and Metabolism, IMED Biotech Unit, AstraZeneca, Gothenburg, Sweden.* [2]*Charles River Laboratories, Montréal, QC, Canada.* [3]*Regulatory Safety, Drug Safety and Metabolism, IMED Biotech Unit, AstraZeneca, Cambridge, United Kingdom.* [4]*Regulatory Safety, Drug Safety and Metabolism, IMED Biotech Unit, AstraZeneca, Gothenburg, Sweden.*

Introduction: Dapagliflozin is a sodium-glucose co-transporter 2 inhibitor for improving glycemic control. Early clinical studies showed more patients with bladder cancer in dapagliflozin than placebo arms. Dapagliflozin was not genotoxic nor carcinogenic in nonclinical studies. Due to regulatory concern that dapagliflozin could promote tumors in patients with pre-existing bladder cancer, we conducted a study in a rodent bladder cancer model.

Experimental Design: Male Sprague-Dawley rats were exposed to 100 or 400 mg/kg N-Butyl-N-(4-hydroxybutyl)-nitrosamine (BBN) po for 6 weeks. After a 2 week washout, 3 groups with 50 animals from the 100 mg/kg BBN cohort were exposed to vehicle control, dapagliflozin 0.5 mg/kg/day or 3% uracil in diet for 26 weeks and 2 groups with 50 animals each from the 400 mg/kg BBN cohort received vehicle control or dapagliflozin 0.5 mg/kg/day, also for 26 weeks.

Methods: Urinary bladders were examined microscopically for the presence of urothelial hyperplasia, papilloma and carcinoma.

Results: Dapagliflozin gave exposures 7-fold to human AUC. There was a slight increase in urothelial hyperplasia in 100 mg/kg BBN animals treated with dapagliflozin compared to controls. Uracil treated animals had increased incidence of urothelial carcinoma compared to control. Animals treated with dapagliflozin had no increased incidence or invasiveness of tumors compared to controls after pretreatment with either 100 or 400 mg/kg BBN.

Conclusion/Impact Statement: Dapagliflozin does not act as a tumor promoter or progressor in rodent bladder cancer at exposures 7-fold above human AUC.

64

Step Sectioning Protocol for Comprehensive Evaluation of Cardiac Valves When Using a Mouse Model

Maureen O'Brien, Elaine Edmonds, Lauren Kuhn, Robert Jacoby.

Charles River Laboratories, Frederick, MD, USA.

Introduction: Cardiac valves are essential for normal transcardiac blood flow and are vulnerable to test article-related changes. However, routine histologic sectioning for standard toxicologic cardiac evaluation in mice may not necessarily include sufficient cardiac valve tissue to detect valvular changes if present. Thus, in studies having a high index of suspicion for possible drug-induced valvulopathy (e.g. class effect), multiple sections of heart can be evaluated to ensure that all valves are adequately examined for test article-related changes.

Experimental Design and Methods: Twelve (12) C57/Bl6 formalin-fixed mouse hearts were submitted for histologic evaluation. Three (3) mice belonged to the control group; the remaining nine (9) mice were divided into three different groups (n=3 mice/group) receiving the test article of a class known to induce valvulopathy. Serial step sectioning was performed on bisected paraffin-embedded hearts at 100 µm intervals. The presence of valve leaflet tissue and valve identity were evaluated to determine how many step sections were necessary for comprehensive cardiac valvular evaluation.

Results: In 10 of 12 mice (83%), portions from all cardiac valve leaflets could be observed within six step sections or fewer.

Conclusion: Bisecting the heart with step sectioning at 100 µm intervals enabled examination of all four cardiac valves within six step sections. Subjectively, slightly smaller step intervals (50–75 um) may also be useful when evaluating mouse cardiac valves.

Impact Statement: Step sectioning bisected mouse hearts at 100 µm intervals generally provides for examination of all four cardiac valves within six step sections or fewer.

65

Novel Off-Target Effect on Urine Concentrating Ability in an Exploratory Rat Toxicity Study

Bruce LeRoy, Michael Foley, Michael Logan.
AbbVie, North Chicago, IL, USA.

Introduction/Objectives: An experimental compound was tested in a rat dose-range finding toxicity study. Following 14 days of once daily administration, overnight urine collection revealed the production of increased urine volumes by treatment group animals compared with animals administered vehicle only. Urinalysis confirmed that urine specific gravity from animals in the mid- and high-dose groups was markedly dilute compared to urine from control animals. An investigative study was performed to understand onset, chronology, and reversibility of the finding, as well as allow collection of endpoints facilitating mechanistic understanding.

Methods, Materials, Experimental Design: Urinalysis, urine volume, water intake, urine/serum osmolality, and serum vasopressin were evaluated in samples from test item dosed rats.

Results: Markedly dilute urine was present following 7 days of administration of test item, but had returned to pre-treatment levels following a 7-day recovery period. Urine volume was increased approximately 2-fold compared with vehicle control animals. Urine osmolality results revealed meaningful differences between treated and control animals. Serum arginine vasopressin levels were increased following 7 days of administration of the test item compared to vehicle animals. Results of an *in vitro* primary pharmacology receptor binding assay demonstrated significant vasopressin receptor 2b antagonism by the experimental molecule.

Conclusion: Results suggest the mechanism underlying the production of increased amounts of dilute urine observed during the dose-ranging toxicity study was impaired renal water resorption due to V2b arginine vasopressin receptor blockade caused by the experimental molecule.

Impact: These data characterize a novel effect on urine concentrating ability in rats.

66

Toxicity of Secondhand Tobacco Smoke on Immune Functions of Alveolar Macrophages in Mice

Minoru Takeuchi[1], Maiko Takasaki[1], Naoko Miwa[1], Yuriko Hirono[1], Yoshiko Tanaka[1], Kent Pinkerton[2].
[1]*Kyoto Sangyo University, Kyoto, Japan.* [2]*UCD, Davis, CA, USA.*

Introduction: Cigarette tobacco smoke is consisted from mainstream tobacco smoke (MTS) and secondhand tobacco smoke (STS). STS is inhaled into the lung by respiration and affect to alveolar macrophage (AM). AM is playing an important role of immune system in the lung. However, the immuno-toxicity of STS on AM is not yet fully demonstrated compared with MTS.

Experimental Design: Mice were exposed to STS of 20 cigarettes/day during 10 days by using STS exposure auto-machine. After STS exposure, AM were obtained by brocho-alveolar lavage (BAL).

Methods and Materials: TLRs expressions, phagocytic activity and reactive oxygen species (ROS) generation were determined by FACS. Expressions of cytokines mRNA were measured by RT-PCR. DNA damage was evaluated by comet assay.

Results: The number of AM was significantly increased in STS exposed mice. Phagocytic activity was significantly inhibited by STS. Expressions of TLRs were significantly inhibited by STS. ROS generations were significantly increased by STS exposure. Expression of TNF-α mRNA was significantly inhibited by STS. DNA damage were significantly increased by STS.

Conclusion: STS exposure caused the change of cell size and intracellular structure in AM. STS induced DNA damage in AM by ROS generation. The phagocytic activity, expressions of TLRs and TNF-α mRNA in AM were decreased by STS. STS indicated toxicity for DNA of AM and inhibition of these immunological functions in AM were mediated by DNA damage.

Impact Statement: Based upon our evaluation, inhibition of immune functions by STS may associated with infection or development of pulmonary disease.

67

Evaluation of the Göttingen Minipig as a Large Animal Model for Otologic Research

Pankaj Kumar[1], Aaron Sargeant[1], Bridget Lewis[1], Jean-Francois Lafond[2].
[1]*Charles River Labs, Spencerville, OH, USA.* [2]*Charles River Labs, Montréal, QC, Canada.*

Introduction: Rabbits, guinea pigs, rats, chinchillas, and dogs are well established animal models for investigating ototoxicity. The use of minipigs as an alternative to nonrodent species has increased in preclinical safety assessment/regulatory toxicity studies. The goal of the present study was to standardize processing of the petrous part of the temporal bone and evaluate the gross and microscopic features of normal Göttingen minipig ear. Comparative aspects with dog are also presented.

Experimental design: Two control male Göttingen minipigs, aged 5 months were used for the present study.

Methods: Left and right petrous portions of the temporal bones were dissected and placed in 10% buffered formalin for a minimum of 72 hours. The ears were decalcified after fixation for 12 days by immersion in formic acid solution. Following decalcification, the tissues were embedded in paraffin, step-sectioned (150 µm intervals), mounted on glass slides, and stained with hematoxylin and eosin.

Results: The study showed remarkable similarities between minipigs and dog ears in terms of spatial arrangement of the ossicular chain, type of epithelium lining the middle ear and the inner ear architecture/histology. Notable differences include long and narrow osseous portion of the external ear canal. Also, the ventral portion of the tympanic cavity is continuous with prominent tympanic bullae which are composed of multiple air filled bony lattice.

Conclusion: The gross morphology and histology of the external, middle, and inner ear of Göttingen swine is presented.

Impact Statement: The Göttingen minipig is a suitable large animal model for otologic research.

68

Anatomy, Histology and Spontaneous and Induced Pathology of the Kidney, and Selected Renal Biomarkers Reference Ranges in the Laboratory Nonhuman Primate

Ronnie Chamanza[1], Stuart Naylor[2], Chidozie Amuzie[3], Vinicius Carreira[4], Jing Ying Ma[4], Alys Bradley[2], Brad Blankenship[5], Kevin McDorman[6], Calvert Louden[3].
[1]*Janssen Pharmaceutical Companies of Johnson & Johnson, Beerse, Belgium.* [2]*Charles River Laboratories, Edinburgh, United Kingdom.* [3]*Janssen Pharmaceutical Companies of Johnson & Johnson, Spring House, PA, USA.* [4]*Janssen Pharmaceutical Companies of Johnson & Johnson, La Jolla, CA, USA.* [5]*Charles River Laboratories, Reno, NV, USA.* [6]*Charles River Laboratories, Wilmington, MA, USA.*

Introduction/Objectives: The nonhuman primate kidney is often a target for large and small molecules in preclinical safety testing, and drug-induced kidney injury is a translational safety concern related to clinical attrition. Toxicologic pathologists must separate drug effects from spontaneous occurrences and normal histology, and in this species, there is a paucity of data on the comparative renal anatomy, physiology, spontaneous pathology, and reference values of traditional renal biomarkers.

Methods: We examined 204 kidneys from male and female Cynomolgus monkeys of 2–3 and 4–6 years, and collected historical control data of background pathology, kidney weights, urinalysis and renal clinical biochemistry analytes.

Results: The functional anatomy of the monkey kidney is similar to that of other laboratory animals and humans, but a few differences exist. Unlike in humans, the macaque kidney is uni-papillate/uni-pyramidal, with a near equivalent cortical-medullary ratio, largely due to a relatively underdeveloped papilla. It may also show unique background findings of unknown pathological significance such as, papillary mineralization, multinucleate cells and cuboidal metaplasia of the parietal cells of the Bowman's capsule. The most common spontaneous pathology findings were interstitial inflammatory infiltrates, although tubular and glomerular findings that may be confused with drug effects were occasionally observed. Kidney weights and some clinical chemistry reference values showed age and sex related variations.

Conclusion and Impact Statement: Taken together, this information improves the use and evaluation of the laboratory primate kidney, and the assessment of the suitability of NHP as an animal model for identifying and characterizing drug-induced renal injury.

69

It's Not Just a Rat Phenomenon: A Case Example of Canine-Specific Thyroid and Pituitary Hypertrophy Secondary to UGT Induction and Increased Thyroid Hormone Metabolism

Sandra De Jonghe[1], Ronnie Chamanza[1], Petra Vinken[1], Geert Mannens[1], Heng-Keang Lim[2], Monicah Otieno[2], Junguo Zhou[3], Gary Eichenbaum[4].
[1]*Janssen Research and Development, Beerse, Belgium.* [2]*Janssen Research and Development, Spring House, PA, USA.* [3]*Janssen Research and Development, Raritan, NJ, USA.* [4]*Johnson & Johnson, New Brunswick, NJ, USA.*

Introduction: Reversible thyroid follicular hypertrophy/hyperplasia and pituitary (pars distalis) hypertrophy were observed in a one-month oral study in dogs; but not in rats or monkeys treated with the same compound. In addition, no effects on circulating thyroid hormones were present in humans.

Methods: To elucidate the mechanism behind the findings, measurements of thyroid hormones and TSH, *ex vivo* analysis of enzyme induction in liver samples, and analysis of plasma concentrations of the compound and its glucuronide metabolite, were carried out.

Results: Moderate to marked dose-related decreases in thyroid hormones and increases in TSH were present in dogs with thyroid hypertrophy. Strong evidence of UGT enzyme induction was demonstrated by a significant decrease in the exposure of the compound on Day 28, increased proportion of glucuronide metabolite relative to parent, and increased thyroxine UGT activity in liver microsomes.

Discussion: Overall, the findings were consistent with the well-described mechanism of thyroxine decrease following UGT induction, with feedback stimulation of TSH and resultant thyroid hypertrophy. Rats and dogs are more susceptible than humans mainly due to the relatively low plasma half-life of their thyroid hormones, and reduced binding affinity to transport proteins, resulting in higher clearance.

Conclusion: Thyroid and pituitary hypertrophy secondary to UGT induction were demonstrated in the dog, and due to the species differences in thyroid hormone metabolism, the findings were not considered relevant to humans.

Impact Statement: The case example demonstrates, that the well-described thyroid and pituitary effects secondary to UGT induction in rats may also occur in the dog.

70

Spice/K2 Induced Encephalopathy and Acute Renal Failure

Eric Chang, Shaheen Fatima, Amina Farooq, Anam Umar, Ifedolapo Odebunmi, Taiwo Ajose, Chinedu Ivonye.
Morehouse School of Medicine, Atlanta, GA, USA.

Introduction: Synthetic cannabinoids (Spice/K2) are poorly understood and contain a mix of substances that may lead to unpredictable side effects. We describe a unique case of synthetic marijuana induced encephalopathy and acute renal failure in a previously healthy male.

Case: A previously healthy 30-year-old man presented with altered mental status via emergency medical services. On presentation, the patient was combative and his vitals were significant for tachycardia. Labs revealed an elevated anion gap (AG 23) metabolic acidosis and acute renal failure (creatinine 5.0, baseline normal). Urine drug screen was negative. Infectious, neurologic, endocrine, and autoimmune studies were unremarkable.

The patient's renal function continued to worsen, with rising creatinine (9.2) and creatinine phosphokinase (CPK 32000) despite aggressive fluid resuscitation. Urine microscopy confirmed muddy brown casts consistent with acute tubular necrosis (ATN). Emergent hemodialysis was initiated with return of mentation to baseline, after which he admitted to one time synthetic marijuana usage. The patient's renal function continued to improve despite discontinuing dialysis (per patient's request), after which he decided to leave against medical advice.

Discussion: Designer drugs such as synthetic cannabinoids may have unpredictable side effects. They are gaining popularity, especially given that they cannot be detected on standard drug screens. Our case is unique in that synthetic marijuana usage led to acute renal failure in the setting of both ATN and rhabdomyolysis, which has previously not been reported. Physicians need to be aware of the growing popularity of synthetic marijuana and learn how to recognize its potential side effects.

71

Histology Atlas of the Developing Mouse Urinary Tract

Sanam L. Kavari[1], Koichi Yabe[2], Mark J. Hoenerhoff[3], John C. Seely[4], Beth Mahler[4], Susan A. Elmore[1].

[1]*NTP, NIEHS, Cellular and Molecular Pathology Branch and National Toxicology Program, Research Triangle Park, NC, USA.* [2]*Medicinal Safety Research Laboratories, Kitakasai, Daiichi Sankyo Co., Ltd., Edogawa-ku, Tokyo, Japan.* [3]In Vivo *Animal Core, Unit for Laboratory Animal Medicine, University of Michigan, Ann Arbor, MI, USA.* [4]*Experimental Pathology Laboratories, Inc., Research Triangle Park, NC, USA.*

Introduction: This atlas aims to provide high resolution color H&E stained images of normal embryonic murine urinary tract development to aid pathologists and biomedical researchers in the identification of abnormalities in embryonic mice and is part of a series of atlases published by the National Toxicology Program on the development of organ systems of the mouse.

Materials and Methods: Embryos from CD-1IGS mice/Cr1: CD1(ICR) were collected for each stage (E10.5-18.5), fixed with paraformaldehyde, then embedded and serial sectionedv. Transverse, sagittal, and coronal sections were obtained for each embryo. Digital images of developmental events were captured.

Experimental Design: A review of relevant literature and histological slides were compared to match developmental events to histological images.

Results: Low and high magnification labeled images and digital scans are provided. Key events in the development of the urinary tract are identified for each stage as well as the developmental origins of urinary tract structures.

Conclusions: An understanding of the normal development of the mouse urinary tract, as provided by this atlas, is important for researchers studying abnormalities of the urinary tract in mice, particularly as a model for human abnormalities.

Impact Statement: The urinary tract develops from the fusion of two distinct systems at the ureteral-bladder junction. We histologically identified the ureteric bud at an earlier stage (E10.5) than in previous literature, indicating earlier initiation of the development of the metanephros. The origins of several urinary structures, notably the urethral sphincter, are not well understood therefore further research is necessary.

72

Anti-Fibrotic Role of miR-214 in Chemically Induced Liver Cirrhosis in Rats

Takeshi Izawa, Takashi Horiuchi, Machi Atarashi, Mitsuru Kuwamura, Jyoji Yamate.

Veterinary Pathology, Osaka Prefecture University, Izumisano, Japan.

Introduction: An increasing number of studies have focused on the role of microRNAs (miRNAs) in liver fibrosis/cirrhosis. miR-214 has recently been considered as a fibrosis-related factor; however, the molecular mechanism in hepatic fibrogenesis remains unknown. Here we investigated the pathological role of miR-214 during progression of thioacetamide (TAA)-induced liver cirrhosis in rats.

Experimental Design: Six-week-old male F344 rats were injected intraperitoneally with TAA (100 mg/kg, twice a week). The liver was collected at weeks 5, 10, 15, and 20.

Method: Hepatic expression of miR-214 was analyzed by microarray, real-time PCR combined with laser microdissection, *in situ* hybridization. The effects of miR-214 overexpression on fibroblastic cells were investigated by *in vitro* transfection using MT-9 cells (rat immature mesenchymal cell line).

Results: miR-214 was highly up-regulated in the fibrotic area of TAA-induced liver lesions, with its expression increasing with the cirrhosis progression. miR-214 overexpression in MT-9 cells under TGF-β1 stimulation resulted in decreased cell number, increased expression of cleaved caspase 3 and decreased expression of α-smooth muscle actin.

Conclusion: The results suggest that miR-214 induces apoptosis and inhibits myofibroblast differentiation of the induced fibroblastic cells.

Impact Statement: Our study revealed an anti-fibrotic role of miR-214 in chemically-induced liver fibrosis/cirrhosis.

73

Modulation of Hepatic Nuclear Receptors in the Progression of Non-Alcoholic Fatty Liver Disease

Xilin Li, Zemin Wang, James Klaunig.
Indiana University, Bloomington, IN, USA.

Introduction: The pathologic progression of non-alcoholic fatty liver disease (NAFLD) involves steatosis, steatohepatitis, fibrosis, cirrhosis and sometimes hepatocellular carcinoma. Nuclear receptors are important in the regulation of normal and pathological liver function in response to chemical and endogenous stress.

Experimental Design: Male C57BL/6 mice were fed either a control diet or a high fat diet for up to 12 months with interim samplings (after 2, 4, 8, 12, 16, 24, 32, and 52 weeks). Livers were processed for both histopathology and transcriptional analysis.

Methods: Measurement of nuclear receptors PPARs, CAR, PXR, LXR, and FXR was performed using gene expression analysis and enzymatic activity.

Results: Chronic feeding of a high fat diet resulted in a progressive increase in steatosis, fibrosis, inflammation and hepatic DNA synthesis. Transcriptomic and pathway analysis after 16 weeks on high fat diet showed an increased activation of PPARα and PPARγ, CAR, and PXR compared to control diet. PPARα was significantly activated (4-fold). PPARγ was slightly elevated while PPARδ was down regulated to 20–40% of control. In contrast, activation of CAR related genes was not as robust as the PPAR related genes. LXR target genes were also elevated correlating with the hepatic steatosis.

Conclusion: In mice, high fat diet modulates the expression of nuclear receptors that correlate with the progression and spectrum of liver pathology.

Impact Statement: NAFLD is a major public health burden. Understanding the changes in nuclear receptors and their downstream drug metabolizing enzymes has importance in susceptibility and treatment of this disease.

74

Analysis of Hemorrhagic Diathesis in Rats Fed a High-Iron Diet

Yohei Inai[1], Takashi Izawa[1], Mutsuki Mori[1], Machi Atarashi[1], Seiichirou Tsuchiya[2], Mitsuru Kuwamura[1], Jyoji Yamate[1].
[1]Veterinary Pathology, Osaka Prefecture University, Osaka, Japan. [2]Sysmex Corporation, Kobe, Japan.

Introduction: Iron overload is well recognized as a cause of oxidant-mediated cellular/tissue injuries, while the effect of iron overload on blood coagulation system has been poorly understood. We previously encountered an unexpected bleeding tendency in some rats fed a high-iron diet. We here investigated the mechanism of hemorrhagic diathesis in rats with dietary iron overload.

Experimental Design: Six-week-old F344/DuCrlCrlj rats were fed a high-iron diet (1% iron; Fe group) or control diet (0.02% iron; control group) for up to 26 weeks.

Methods: Hematological, biochemical, coagulation and pathological examinations, and RNA-sequencing using liver samples were conducted.

Results: In Fe group, serum iron and liver iron increased 3.4-fold and 4.7-fold, respectively. Hemorrhage was observed in 11/47 rats (23.4%) of Fe group; it was found in the nose, tail, skeletal muscle, orbit, lung, thymus, epididymis and peritoneal cavity. Significant prolongation of PT and APTT, decreased activity of coagulation factor II and VII was found in the Fe group, whereas the activity of factor VIII did not change. Expression profile of coagulation factor genes in the liver did not change significantly between control and Fe groups.

Conclusion: Our results suggest that dietary iron overload can cause blood coagulation abnormalities, resulting in hemorrhagic diathesis.

Impact Statement: Iron overload can affect activity of several coagulation factors through vitamin K deficient or other unknown mechanisms, whereas it does not affect the production of coagulation factors.